Electronic Supplementary Material (ESI) for RSC Advances.

Supporting Information

for

A Sustainable Chemistry Solution to the Presence of Pharmaceuticals and Chemicals in the Aquatic Environment- the Example of Re-Designing β-blocker Atenolol

Tushar Rastogi, Christoph Leder, Klaus Kümmerer*

Sustainable Chemistry and Material Resources, Institute of Sustainable and Environmental Chemistry, Leuphana University Lüneburg, C13, DE-21335 Lüneburg, Germany

* Corresponding author email address: Klaus.Kuemmerer@uni.leuphana.de

Table of Contents

Text S1 Supporting Information: Generation of photo-transformation products (photo TPs) of ATL and characteristics of UV lamp

Test procedure

Photolysis: ATL was dissolved in ultrapure water for direct photolytic experiments with no pre-treatment in order to exclude any other constituents that could interfere with the formation of derivatives and/or to avoid the initiation of scavenger effects of any absorbing or photosensitizing chemical or other species during degradation. Photolysis of ATL was performed in a 1L batch photo reactor irradiated by 150 W medium-pressure mercury lamp (TQ150, UV Consulting Peschl, Mainz) with Ilmasil quartz immersion tube as described elsewhere in detail.[1,2] The batch photo reactor was provided with constant stirring and the temperature in the reactor was maintained between 18-20 °C through temperature control by a circulating cooler (WKL230, LAUDA, Berlin).

Sampling: In order to monitor the kinetics of transformation and mineralization of ATL, samples (20 mL) were collected after 2, 4, 8, 16, 32, 64, 128 and 256 min of irradiation time respectively. The primary elimination of ATL and formation of photo-transformation products (photo-TPs) was monitored by HPLC-UV-Vis and LC-ESI-MS^n (ion-trap), respectively.

Characteristics of UV lamp

According to the manufacturer, the total radiation flux Φ from 200 nm to 600 nm is 47 W m^{-2} and the maximal intensities for whole spectral distribution were at following wavelengths

Table S1 Supporting Information: The maximal intensities at following of medium pressure mercury lamp TQ 150 (as provided by manufacturer)

Wavelength (nm)	**Intensities (W m^{-2})**
254	4.0
265	1.4
302	1.8
313	4.3
366	6.4
405/408	3.2
436	4.2
546	5.1
577/579	4.7

Text S2 Supporting Information: Analytical method parameters for chromatography and identification of derivatives (photo-TPs) of Atenolol (ATL)

HPLC method for the elution of ATL:

A Shimadzu Prominence HPLC system (Duisburg, Germany) was used to measure the elimination of ATL. A NUCLEODUR® RP-C18 (CC 125/4 100-5µm C18 ec) column and mobile phases consisting of 0.1 % formic acid in ultrapure water (CH_2O_2: solution A) and 100 % acetonitrile (CH_3CN: solution B) were used for the chromatographic separation. The flow rate, column oven temperature and injection volume was set to 0.5 mL min^{-1}, 25 °C and 50 µL, respectively. ATL eluted at retention time [t_R] 10.9 min. High linearity correlation [$r^2 \geq$ 0.9999] was obtained for calibration curve range from 0.0978 µg mL^{-1} to200 µg mL^{-1}. A gradient flow method was used as describe in Table S2.

Table S2 Supporting Information: Gradient flow condition used to achieve the desired separation

Time (min)	%B (Acetonitrile)
0.01 to 2 min	1
2 to 27 min	1% - 65% B
27 to 29 min	65% - 20% B
29 to 30 min	20% - 1% B
30 to 32 min	1% B
32.01	stop

MS parameter for the identification of derivatives of ATL:

An Agilent LC 1100 series coupled to a Bruker Daltonic Esquire 6000+ ion-trap mass spectrometer (IT-MS) with electrospray ionization (ESI) interface was used for identification and structure elucidation of ATL and the formed derivatives (photo-TPs). The above mentioned LC parameters were used while the MS parameters were optimized for ATL [m/z

267.1] by direct infusion of a 10 µg mL^{-1} standard at a flow rate of 4 µL min^{-1} through a syringe pump. The mass spectrometer was operated in positive polarity. The photo-TPs were identified by comparing 0 min samples (i.e. ATL) as reference with other samples. Their supposed structures were elucidated by interpreting the MS^n spectra.

Table S3 Supporting Information: The operating parameters of the ESI and ion-trap (Bruker 6000) of the LC-ESI-IT-MS^n

Parameters	Metoprolol
Dry gas temperature	350°C
Nebulizer pressure	30 psi
Dry gas flow	10 L min^{-1}
end plate Offset	-500 Volt
capillary voltage	-3583 Volt
skimmer	40 Volt
capillary exit	111. 0 Volt
octopole one	12.00 Volt
octopole two	1.70 Volt
trap drive	38.2
lens one	-5.0 Volt
lens two	-60 Volt
target mass	267 m/z
maximum accumulation time	200 ms
scan range	40 m/z - 1000 m/z
fragmentation amplitude	1

DOC measurement:

Dissolved Organic Carbon (DOC) was measured by Shimadzu TOC-V_{CPN} analyzer equipped with an ASI-V auto sampler. DOC was measured according to ISO 8245: 1999 guideline[3] using a Shimadzu TOC-VCPN analyzer equipped with an ASI-V auto sampler. Samples were filtered with the syringe filter (Chromafil® Xtra PES 45/25, Macherey Nagel, Düren, Germany) of 0.45µm pore size prior to DOC measurement.

Text S3 Supporting Information: Principles and procedure of the investigated aerobic biodegradation tests

The aerobic biodegradability of ATL and its derivatives was investigated according to the OECD guidelines through Closed Bottle test [CBT] 301D[4] and Manometric Respiratory Test [MRT] 301 F.[5]

In CBT the concentration of the test compound was adjusted to 5 mg L^{-1} Theoretical Oxygen Demand without nitrification ($ThOD_{NH3}$) for untreated samples. The sample volume of post-treated solutions was increased according to DOC elimination during photodegradation treatment in order to have sufficient organic carbon related to the LOQ (limit of quantification) of the method used for the measurement of the endpoint parameter (oxygen consumption/oxygen concentration in test solution).

The test consisted of four different series that were run in duplicates, respectively. The blank series contained only mineral medium and inoculum. The quality control series contained readily biodegradable sodium acetate at a concentration corresponding to 5 mg L^{-1} $ThOD_{NH3}$, mineral medium and inoculum. The actual test series contained the respective test substance, mineral medium and inoculum. The fourth series was the toxicity control which contained the test compound and sodium acetate at concentrations corresponding to 5 mg L^{-1} $ThOD_{NH3}$ each. The toxicity control monitors inhibitory effects due to the toxicity of test substances against the inoculum's bacteria and in order to allow for the recognition of false negative results. All the test vessels were inoculated with 2 drops of the effluent from a local municipal STP (AGL Lüneburg, Germany, 144,000 population equivalents).

The aerobic biodegradation in CBT was monitored for 28 days by measuring oxygen concentration in the test vessels with Fibox 3 (Fiberoptical oxygen transmitter) (PreSens, Regensburg, Germany).[6] For quality assessments pH was measured at 0 and 28 days.

MRT was conducted using the OxiTop® Control OC110-system (WTW GmbH, Weilheim, Germany) for monitoring the microbial oxygen consumption through CO_2 production during

the aerobic biodegradation. These measuring heads contained sodium hydroxide which removes the CO_2 from the gas phase. The removal of CO_2 results in a decrease in pressure in test vessels which corresponds to the oxygen consumption which is due to biodegradation. The scheme was equivalent to that of CBT, except that the sample concentration was adjusted to 30 mg L^{-1} ThOD and 80 mL of inoculum were added to 1 L of test solution as required by test guidelines. Furthermore, an additional sterile control for the assessment of abiotic degradation was applied. The sterile control contained the test substance and sodium azide with no inoculum. A more detailed description of the testing procedures can be found elsewhere.[1,2]

The samples after 0 min, 32 min and 256 min of photolysis were tested in CBT while samples after 0 min, 64 min and 256 min were tested in MRT. The difference in the irradiation time of samples for both tests was due the difference in the kinetics of formation of the derivatives. This difference in the kinetic was due to the different starting concentration of ATL in the treatment. Table S4 summarizes the composition of the aerobic biodegradation test series in CBT and MRT.

Substances showing at least 60% degradation (based on oxygen consumption) in these tests are classified as readily biodegradable according to test guideline[7] and therefore are expected not to being accumulated in the aquatic environment.[8]

Table S4 Supporting Information: Composition of the aerobic biodegradation test series in the CBT (1-4) and MRT (1-5)

Test series	1 Blank	2 Quality control	3 Test compound	4 Toxicity control	5 Sterile control
Mineral medium	+	+	+	+	+
Inoculum	+	+	+	+	
Test substance			+	+	+
Sodium acetate		+		+	
Sodium azide					+

Text S4 Supporting Information: Detailed description and output from various *in silico* models used in the present study.

Photo-TPs: The photodegradation pathway of ATL and resulting photo-TPs ("derivatives") products was established by using a combination of chemical analysis (LC-ESI-ion-trap-MS/MS structure elucidation, see above, S2) and *in silico* prediction by the software MetaPC (Version 1.8.1, MultiCASE Inc., Beachwood, USA[9], Table S5, SI) using its photo-degradation dictionary. *In silico* predictions were compared to the corresponding MS^n spectra measured by LC-ESI-MS/MS (ion-trap).

The dictionary is a compilation of known rules for photo reactions of chemicals. Generally, the dictionaries of MetaPC software are based on a library of known pairs of target and transform sequences. Meta program uses respective dictionaries to predict the transformation of chemicals under a set of different conditions such as mammalian metabolism, aerobic and anaerobic degradation and photodegradation. The structures of investigated molecules are scanned for their target sequences which are gradually replaced by the relevant transform sequences of the respective dictionary to create a set of predicted TPs.[9] The photodegradation dictionary of the MetaPC software is loosely divided into 9 large subdivisions which consist of approximately 1200 transformations in total. The photodegradation dictionary module was validated with 40 known industrial chemical products and had a hit/miss ratio of higher than 92%. MetaPC is an efficient model for the evaluation of the photo-induced degradation processes that take place in diluted conditions in oxygenated aqueous solutions.

Biodegradability: The *in silico* models used to predict the aerobic biodegradability of ATL and its derivatives (photo-TPs) are summarized in Table S5. As all *in silico* models and approaches have their limitations, therefore a combination of several software packages that rely on different data sets and underlying algorithms/statistics has been applied ("*in-silico* testing battery"). The ready biodegradability of ATL and its derivatives was predicted based

on data for OECD 301C MITI-I test (Ministry of International Trade and Industry, Japan)[7], which is generally not fully comparable to CBT and MRT, as models for the CBT are not available. However, these predictions can provide at least an orientation towards identifying certain structural alterations in the derivatives molecules which would modulate their biodegradability.

The OASIS Catalogic models predict the ready biodegradability as a numerical value between 1 and 0. A numeric value of 1 corresponds to 100% biodegradation and 0 represents 0% biodegradation while numeric value of 0.6 corresponds to 60% biodegradation which is the pass criterion for ready biodegradability under MITI-I tests conditions. The output from BIOWIN models is also a number between 0 and 1 which can be interpreted as indicating ready biodegradation if the value is higher than 0.5.

Toxicity: Toxicity against environmental bacteria (against *Vibrio fischeri* an often used test organism for this purpose), mutagenicity and genotoxicity for ATL and its derivatives (photo-TPs) were predicted *in silico* by various models of OASIS Catalogic (Laboratory for Mathematical chemistry, Bulgaria), CASE Ultra (MultiCASE Inc., USA) and Leadscope software (Leadscope, Inc., USA), which are listed in Table S5. Leadscope software was used with training sets from 2012 SAR Genetox Database as provided by Leadscope.[10] The mutagenicity was predicted by *in vitro* model for bacterial mutagenicity of OASIS Catalogic. This model identifies chemicals, which are able to elicit mutagenicity as a result of interaction with DNA of *Salmonella typhimurium* or *Escherichia coli*. Micronucleus formation (A7S) for genotoxicity and chromosome aberration (A7U) and mutagenicity Ames (A2H) models for mutagenicity were used from Case Ultra software for prediction.

CASE Ultra, Leadscope and OASIS Catalogic software provide positive, negative and out of domain (OD) estimations for the selected models. OD means that the test chemical is not included in the applicability domain of the applied model. In such cases there are no

predictions made or even if provided by the software they should be discarded. The advantage of Case Ultra software is that it does not only calculate the activity but also evaluates the data and predict the moieties of the molecule which could be responsible for the activating and deactivating activity. Often CASE Ultra software provides alerts for all its selected models like 'Inconclusive' and Inconclusive with asterisk symbol (*). 'Inconclusive' alert means that a significant portion of the test chemical is covered by unknown structural fragments and Inconclusive with asterisk symbol (*) means both positive and deactivating alerts were found in the same molecule. In both cases therefore a clear result cannot be provided.

All the *in silico* models used in the study have validated databases and training sets. More information about their databases, training sets and their validity criteria can be easily found elsewhere in the references provided in Table S5 for each model. Generally, the structures of chemical species are scanned by the software against these validated databases of the model, and the software calculates the activity and predicts the output in the form of alerts for that corresponding activity. The above mentioned models and software are described in detail elsewhere.[1,2,11] Table S5 below enlisted all the *in silico* software and their respective models used in the present study.

Table S5 Supporting Information: List of *in silico* software and their respective models used for the prediction of photodegradation products, ready biodegradability and toxicity of ATL and its photo-TPs.

Activity	QSAR Software	Models	End points	References
Photodegradation products	METAPC v 1.8.1	Photodegradation	Photoproducts of chemicals under natural-like conditions	[9]
Biodegradation	CASE Ultra v.1.4.5.1	MITI-I test (OECD 301C, module AU6)	Ready biodegradability according to MITI-I test	[12]
	EPI Suite (EPIWEB 4.1)	BIOWIN 6	Nonlinear regression models predicting the Ready biodegradability according to MITI-I test	[13]
	Catalogic v 5.11.6 TB (OASIS)	CATABOL 301C model	Ready biodegradability according to MITI-I test	[14]
		CATALOGIC 301C models	Ready biodegradability according to MITI-I test	
Toxicity	CASE Ultra v.1.4.5.1 (MultiCASE Inc.)	Human carcinogenicity (A0J)	Carcinogenicity	[12,15]
		Micronucleus formation in vivo composite (A7S)	Genotoxicity	
		Chromosome aberration in vitro composite (A7U)	Mutagenicity	
		Mutagenicity Ames (A2H)	Mutagenicity against *Salmonella Typhimurium*	
		Microtox toxicity environmental bacteria (AUA).	Bacterial toxicity	
	Leadscope V. 3.0.11-1	Bacterial mutagenesis (BM) model	Mutagenicity as a result of interaction with DNA of *Salmonella Typhimurium* or *Escherichia coli*	SAR Genotox Database 2012 [10]
		Mammalian mutagenesis (MM)	Mutagenicity	
		In vitro chromosome aberration (IVCA)	Mutagenicity	
		In vivo micronucleus (IVMN)	Genotoxicity	
	Catalogic v 5.11.6 TB (OASIS)	*in vitro* Ames model	Mutagenicity against *Salmonella Typhimurium*	[14]

Text S5 Supporting Information: Detailed description of the drug-likeness prediction software QikProp 3.8.

The software package QikProp 3.8 developed by Jorgensen[16] was used to predict drug-likeness of the biodegradable derivatives (photo-TPs) of ATL. QikProp is a quick, accurate, easy-to-use absorption, distribution, metabolism, and excretion (ADME) prediction program. QikProp software (part of Schrödinger software package, Schrödinger, Germany) predicts the drug-likeness through the calculation of various physically significant descriptors and pharmaceutically relevant properties of organic, ligand-like molecules. The software database has ~710 compounds including about 500 drugs and related heterocycles.[17] In addition to predicting molecular properties, QikProp provides ranges for comparing a particular molecule's property with those of 95% of known drugs. Below the properties or descriptors used to predict the drug-likeness of the biodegradable derivatives (photo-TPs) of ATL are explained in detail.

The drug-likeness of chemical molecule is predicted through the **'#stars'** property. The **'#stars'** property of QikProp measures the number of property or descriptor values that fall outside the 95% range of similar values for known drugs. The properties and descriptors which are included in the determination of #stars are mentioned in the technical information manual of QikProp software.[17] The range for #stars predictions is between 0-5. A large number of stars suggest that a molecule is less drug-like than molecules with few stars.

The **RuleOfFive** number gives the number of violations of Lipinski's rule of five.[18] Compounds that satisfy this rule-of-five are considered drug-like. The rules are: molecular weight of molecule < 500, octanol/water partition coefficient (log $P_{o/w}$) < 5, hydrogen bond donors ≤ 5, hydrogen bond acceptors ≤ 10. The **RuleOfThree** number is the counting of violations of Jorgensen's rule of three. Compound that satisfy this rule-of-three are considered as orally available. The three rules are: aqueous solubility (log S) > -5.7, apparent

Caco-2 cell permeability > 22 nm/s, number of likely metabolic reactions < 7. Molecules satisfying these rules are considered orally available. Compounds with fewer (and preferably no) violations of both rules are more likely to be considered drug-like and orally available molecule, respectively.

Text S6 Supporting Information: Results of photolysis and generation of derivatives (photo-TPs) of ATL.

ATL solutions (initial concentration varying from 10 to 60 mg L^{-1}) were exposed to UV light for 256 min. This resulted in the complete primary elimination of the parent compound with incomplete mineralization as measured according to HPLC-UV and DOC analysis, respectively. New peaks were observed in the total ion chromatogram (TIC) during LC-MS analysis at different irradiation time points confirms the formation of derivatives. Several derivatives (photo-TPs) of ATL identified during the photolysis have already been reported in literature.[19–27] New derivatives that have not yet been reported were identified as well. The retention time (t_R), molecular formula, extracted ion chromatogram (EIC) and the MS^2 fragmentation pattern of ATL and its derivatives (photo-TPs) are provided in detail in SI Table S8.

According to LC-MS/MS data, several identified derivatives (photo-TPs) had the same respective nominal mass with different retention times. The retention time dives some information of the polarity of the individual compound. The chromatographic material was a non-polar C18 material. Therefore, lower retention times indicate a higher polarity of the analyte which may in some cases also correlate with a lower log P_{ow}. In most cases these derivatives exhibited the same MS^2 fragmentation pattern, indicating the possibility of formation of constitutional isomers. The same phenomena of the formation of constitutional isomers were reported earlier.[20,21,24]

The kinetics of the appearance/disappearance of derivatives (photo-TPs) formed during photolysis was monitored and is illustrated in Figure S1. Generally, the peak area does not precisely indicate the concentration of the respective derivative in the photodegraded mixture as its molar extinction coefficient and ionization rate is not known. However, determination of

relative change of the concentration of individual derivatives during photolysis is possible thereby.

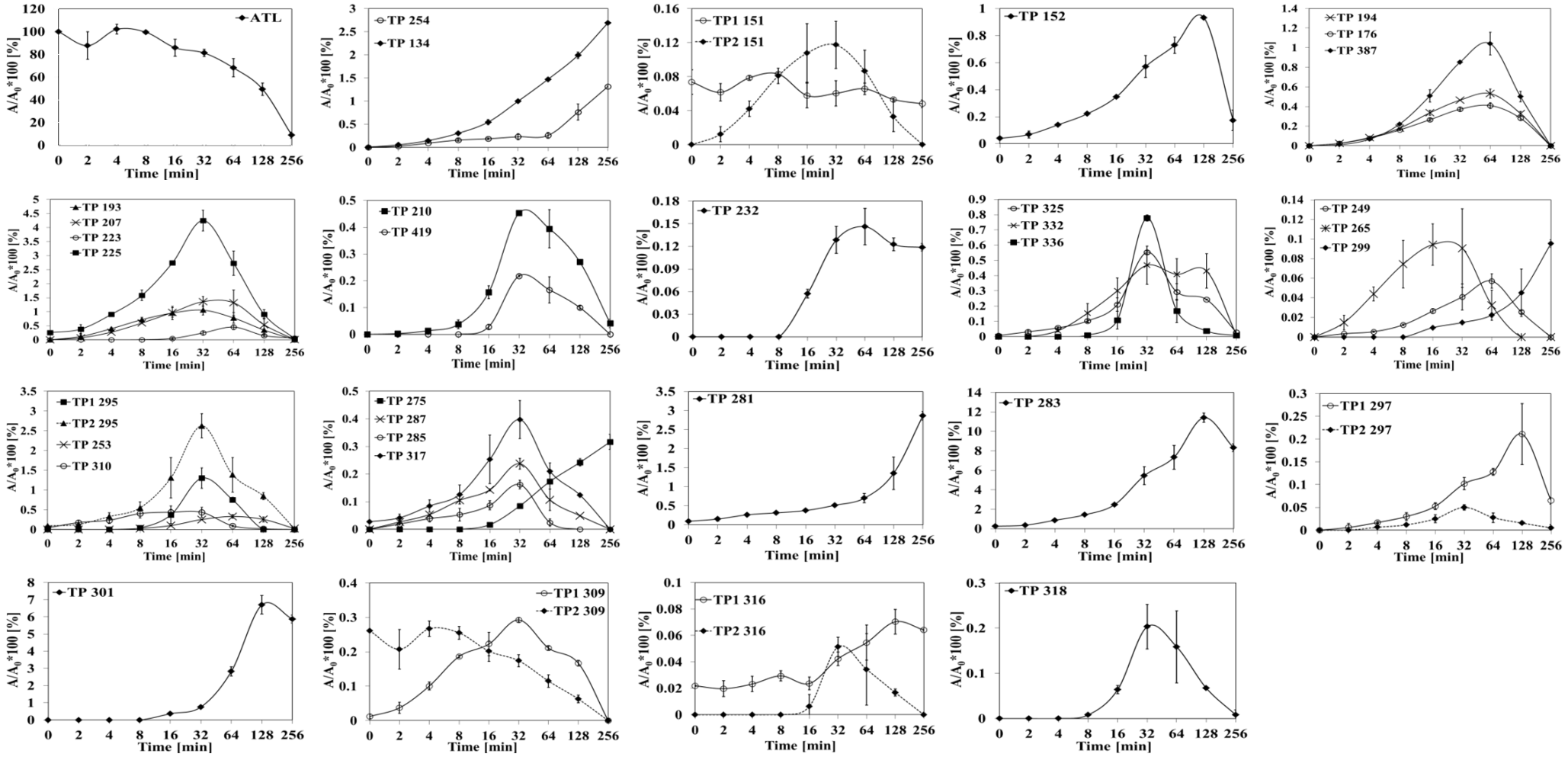

Figure S1 Supporting Information: Appearance/disappearance of peak area of the derivatives (photo-TPs) of ATL during photolysis measured by LC-ESI-MS in positive mode. (Initial concentration of ATL = 10mg L^{-1}; n = 2) (A/A_0 as A is the peak area of derivatives and A_0 is the peak area of ATL at 0 min)

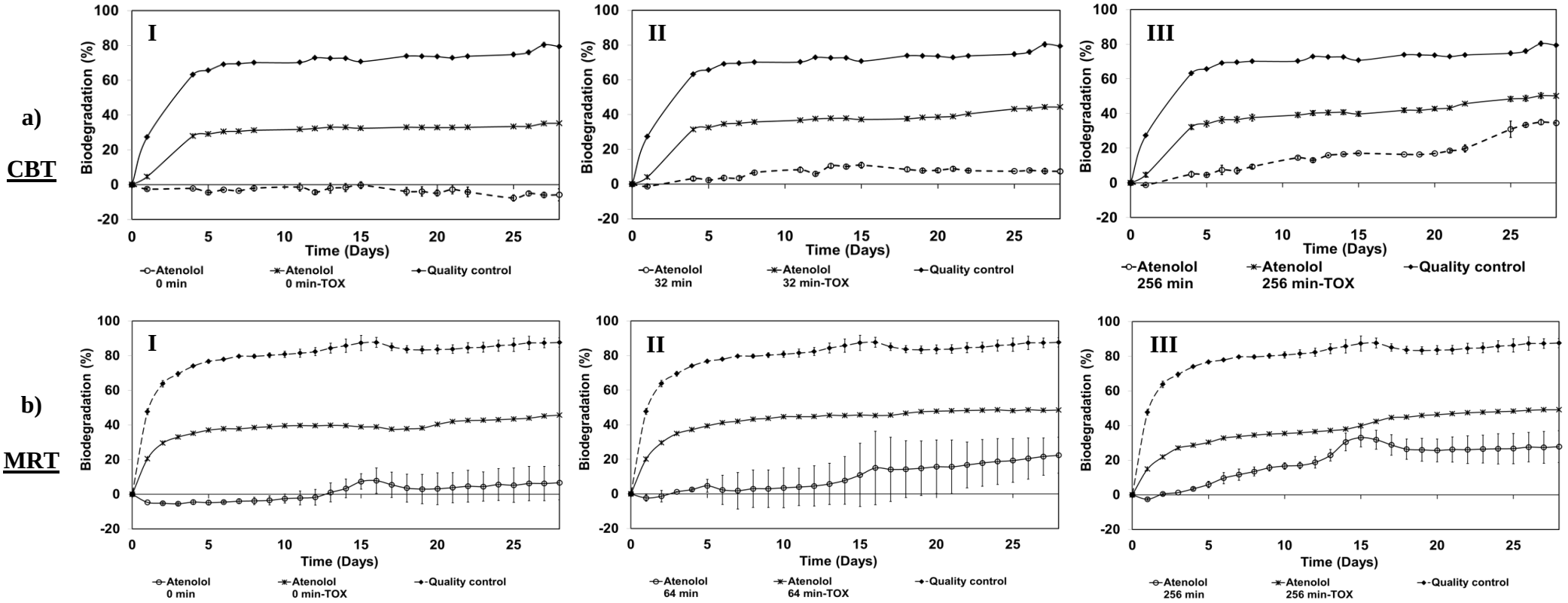

Figure S2 Supporting Information: Aerobic biodegradation results of ATL and its derivatives (photo-TPs) in: a) CBT after photolysis at **I**- 0 min, **II**- 32 min and **III**- 256 min [C_0 =10 mg L^{-1}; n = 2]; b) MRT after photolysis at **I**- 0 min, **II**- 64 min and **III**- 256 min [C_0 = 60 mg L^{-1}; n = 2].

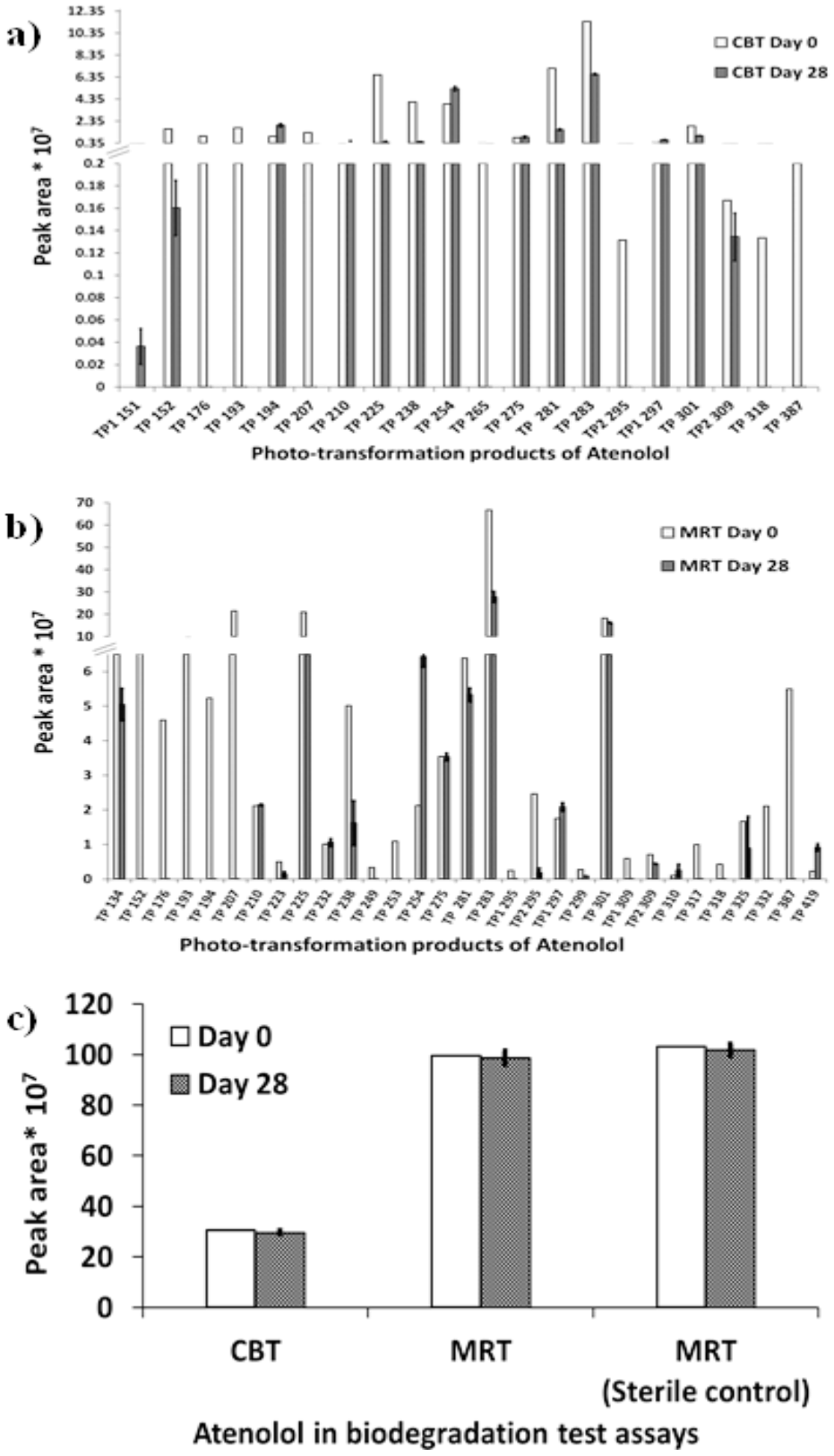

Figure S3 Supporting Information: LC-MS analysis of biodegradation test samples for photo TPs at the beginning and the end of the tests, respectively: a) CBT; b) MRT; c) Atenolol in CBT and MRT.

Table S6 Supporting Information: Summary of the results of investigated aerobic biodegradability test for Atenolol and its derivatives mixture

Biodegradation test	**Test Sample**	**Biodegradation after 28 d [%]**	**DOC removal [%]**	**Derivatives (photo-TPs) identified to be biodegraded**
CBT	0 min	-6 ± 4 %	-	TP 134; TP 152; TP 176; TP 193; TP 207; TP 225; $TP_{1\&2}$ 238; TP 265; TP 281; TP 283; TP_2 295; TP 301;TP_2 309; TP 318; TP 387
	32 min	8 ± 1 %	-	
	256 min	35 ± 2 %	-	
MRT	0 min	7 ± 10 %	9 %	TP 134; TP_1 151; TP 152; TP 176; TP 193; TP 194; TP 207; TP 223; TP 225; $TP_{1\&2}$ 238; TP 249; TP 253; TP 281; TP 283; TP_2 295; TP 299; TP 301; $TP_{1\&2}$ 309; TP 317; TP 318; TP 325; TP 332; TP 387
	64 min	22 ± 10 %	23 %	
	256 min	28 ± 9 %	34 %	

Table S7 Supporting Information: *In silico* drug-likeness prediction of the biodegradable derivatives (photo-TPs) of Atenolol through the ADME prediction software QikProp

Substance and Photo-TPs	Drug-likeness [#star]*	No. of violation of Lipinski's rule of five‡	No. of violation of Jorgensen's rule of three‡
ATL	0	0	0
TP 176	1	0	0
TP 193	0	0	0
TP 194	0	0	0
TP 207	0	0	0
TP 210	0	0	0
TP 223	0	0	0
TP 225	0	0	1
TP 238	0	0	0
$TP_{1\text{-}7}$ 283	0	0	1
TP_1 295	0	0	1
TP_2 295	0	0	0
TP 299	0	1	2
TP_1 301	1	0	1
TP_2 301	1	0	1
TP_3 301	0	0	1
TP_4 301	0	0	1
TP_5 301	1	0	1
TP_6 301	0	0	1
TP_2 309	0	0	1
TP 317	3	0	2
TP 318	2	0	1
TP 325	0	0	1
TP 332	2	1	2

***** predict the drug-likeness in range of 0-5, 0 suggests that molecule is more drug-like while 5 suggest less drug-likeness of the molecule. ‡ Molecules with fewer (and preferably no) violations are more likely to be considered as drug-like and orally available molecules, respectively.

Table S8 Supporting Information: The proposed structures of the fragments formed during the MS^2 fragmentation for Atenolol and its derivatives (photo-TPs), not all mesomeric structures shown (References: if already documented in literature)

m/z	Retention time	Precursor/ Product ion	Structure	References
ATL 267.1	10.9	$[M+H]^+$	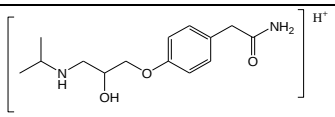	20,24,27
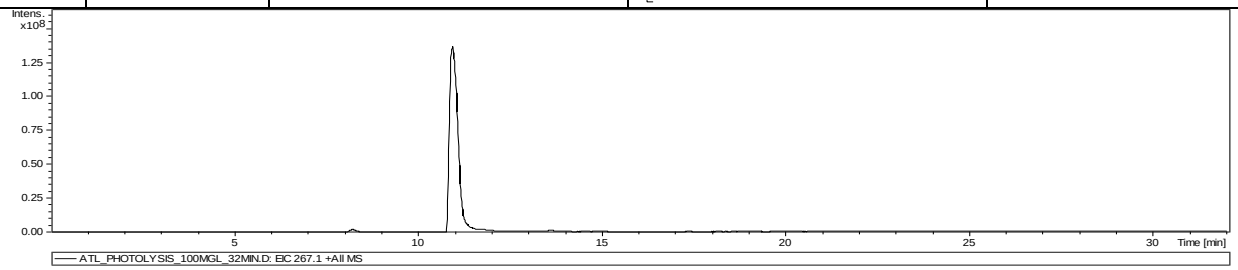				
MS^2				
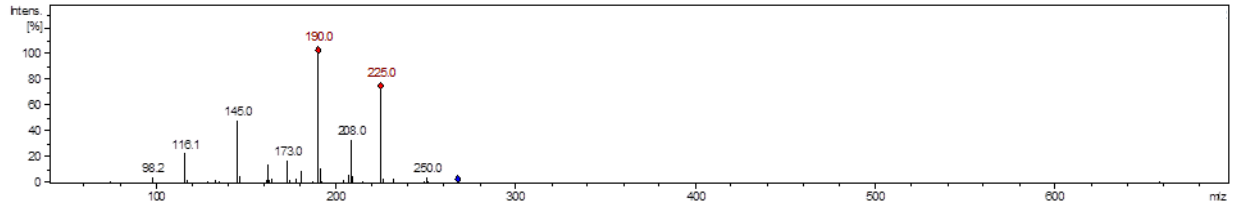				
250.0		$[M+H-NH_3]^+$	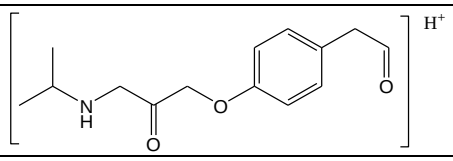	
225.0		$[M+H-C(CH_3)_2]^+$	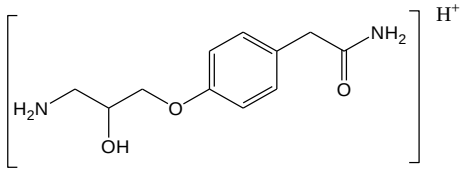	
208.0		$[M+H-NH_2C(CH_3)_2]^+$	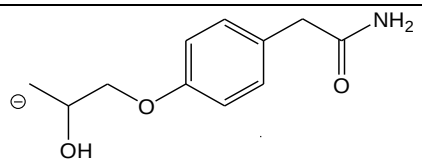	
190.0		$[M+H-NH_2C(CH_3)_2-H_2O]^+$	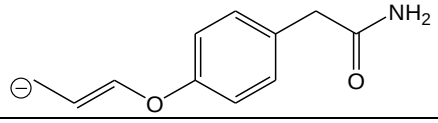	
173.0		$[M+H-NH_2C(CH_3)_2-H_2O-NH_2]^+$	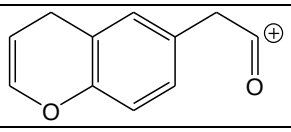	
145.0		$[M+H-NH_2C(CH_3)_2-H_2O-CO-NH_2]^+$	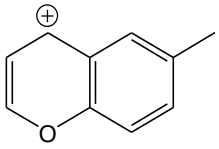	

116.1	[M+H-$HOC_6H_4CH_2CONH_2$]$^+$	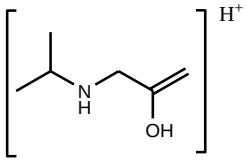
98.2	[M+H-$HOC_6H_4CH_2CONH_2$-H_2O]$^+$	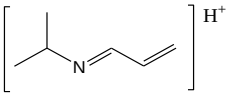

TP 134

m/z	Retention time	Precursor/ Product ion	Structure	References
134.1	2.0	[M+H]$^+$	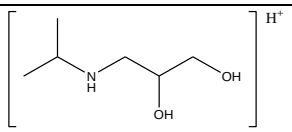	20,24,26,27 MetaPC software

MS^2

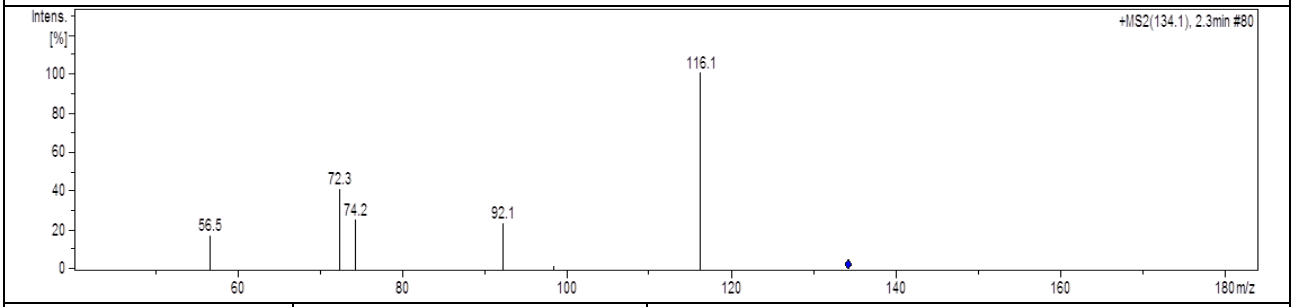

116.1	[M+H-H_2O]$^+$	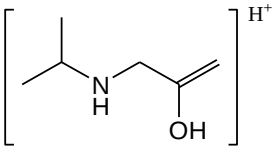
92.1	[M+H- $CH(CH_3)_2$]$^+$	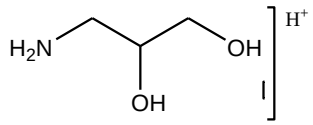
74.2	[M+H-H_2O- $CH(CH_3)_2$]$^+$	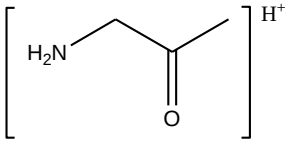
72.3	[M+H-H_2O-$CH2(CH_3)_2$]$^+$	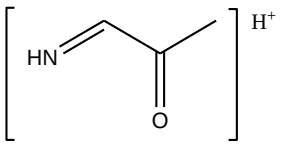

TP 151

m/z	Retention time	Precursor/ Product ion	Structure	References
151.1	9.1 min and 9.5 min	$[M+H]^+$	TP_1 151 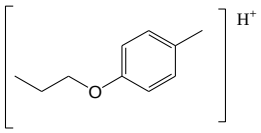 TP_2 151 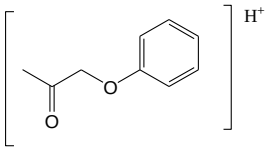	

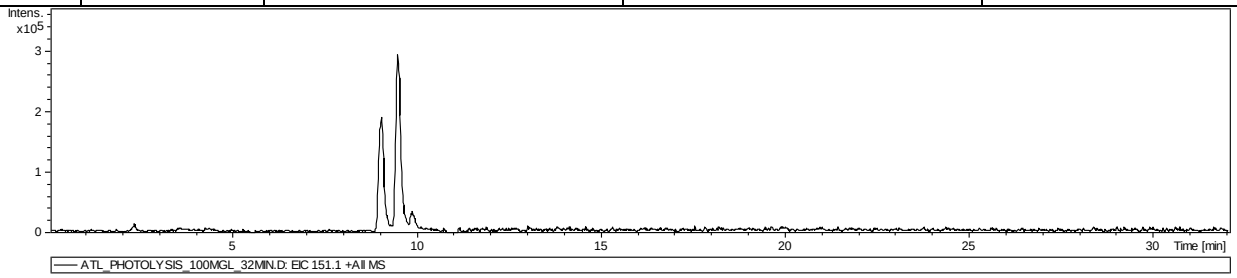

MS^2 of TP_1 151

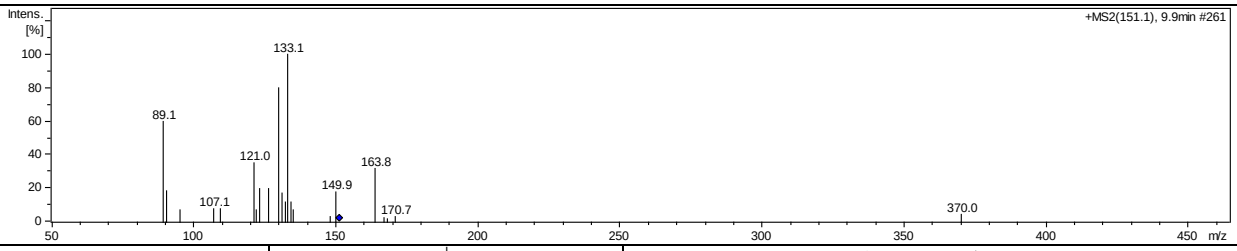

133.1	$[M+H-CH_3]^+$	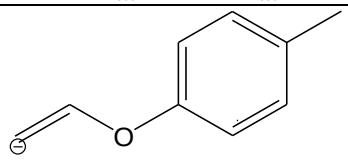
121.0	$[M+H-2CH_3]^+$	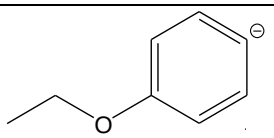
107.1	$[M+H-CH_3CH_2CH_3]^+$	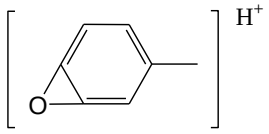

MS^2 of TP_2 151

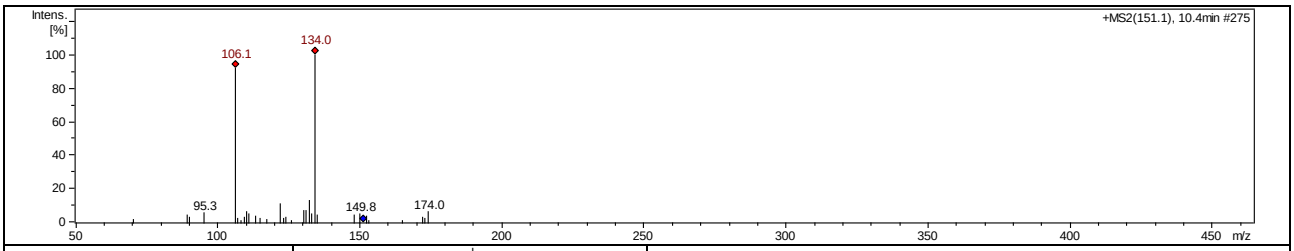

134.0	$[M+H-H_2O]^+$	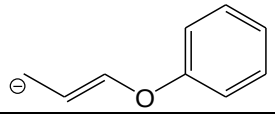
106.1	$[M+H-CH_3CHO]^+$	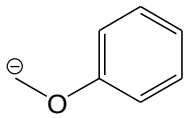
95.3	$[M+H-CH_3COCH_3]^+$	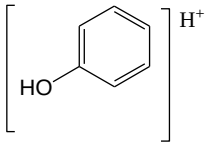

TP 152

m/z	Retention time	Precursor/ Product ion	Structure	References
152.1	11.7	$[M+H]^+$	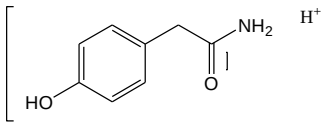	19,20,23,24,26,27 MetaPC software

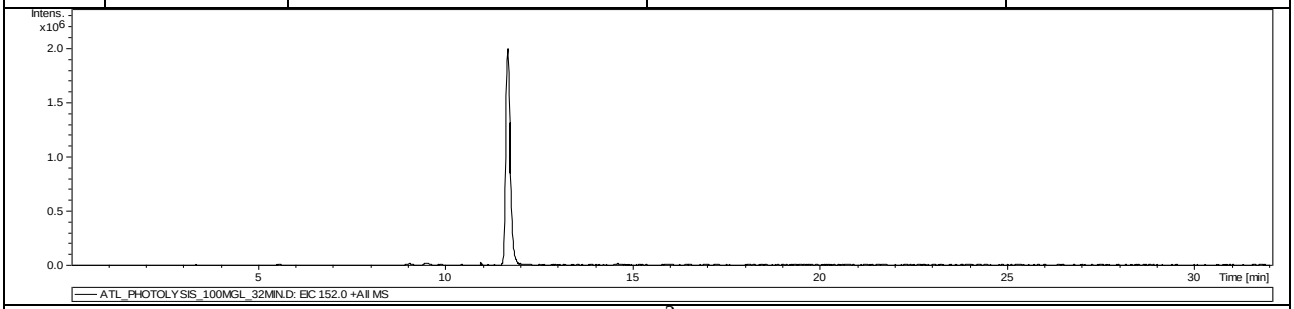

MS^2

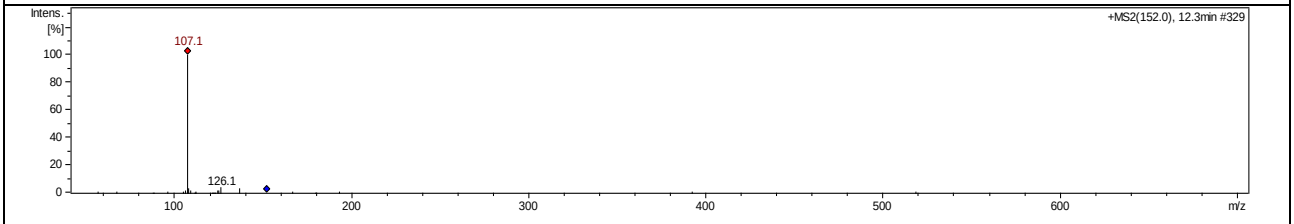

107.1	$[M+H-CHONH_2]^+$	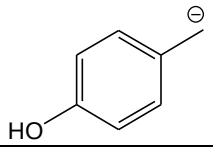

TP 176

m/z	Retention time	Precursor/ Product ion	Structure	References
176.0	12.0	$[M+H]^+$	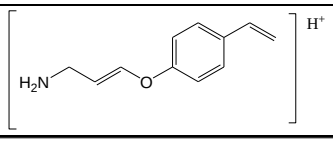	

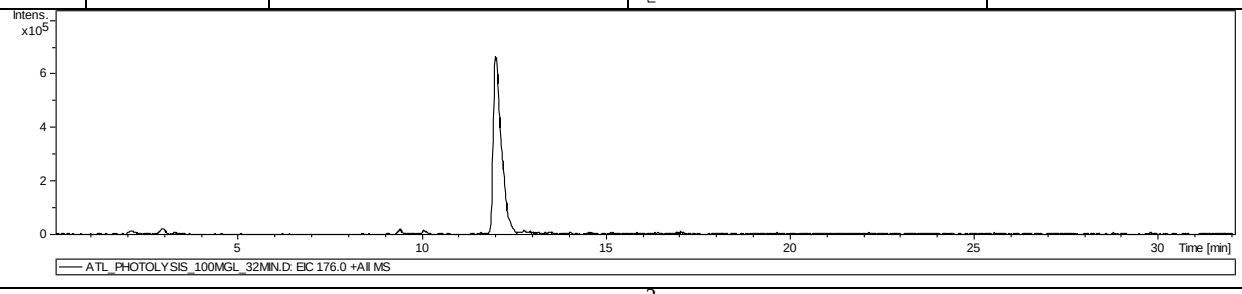

MS^2

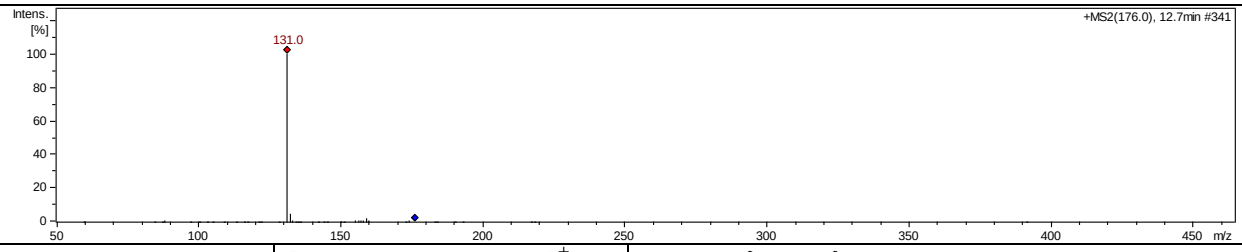

131.0	$[M+H-CH_3CH_2NH_2]^+$	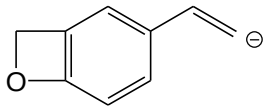

TP 193

m/z	Retention time	Precursor/ Product ion	Structure	References
193.1	9.5 min	$[M+H]^+$	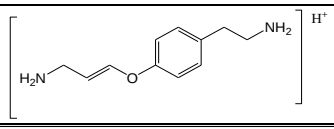	

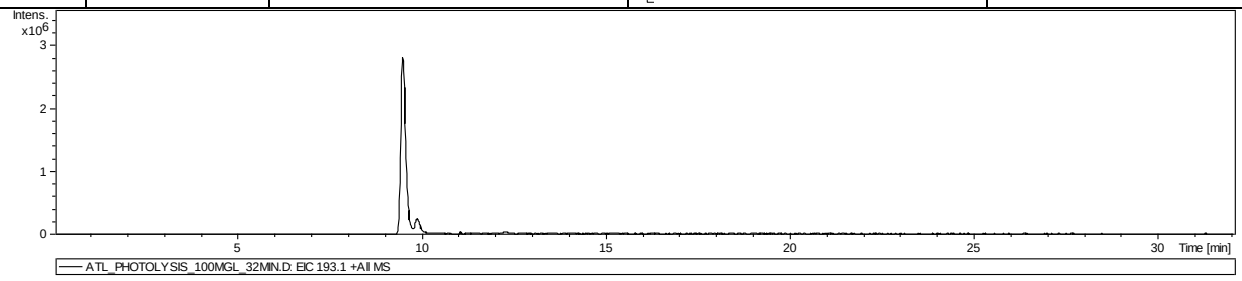

MS^2

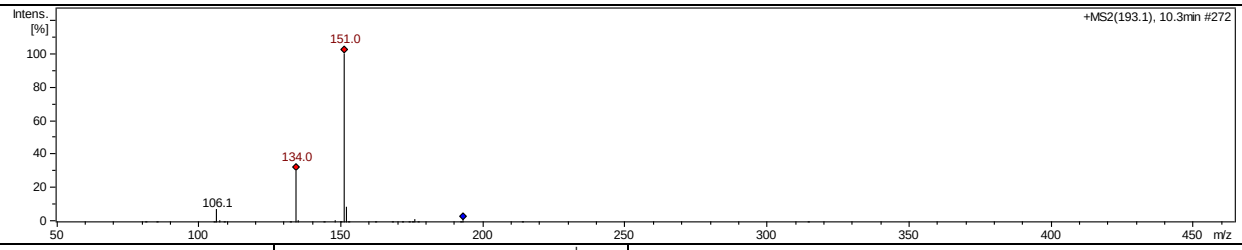

151.0	$[M+H-NH_3-CH_3NH_2]^+$	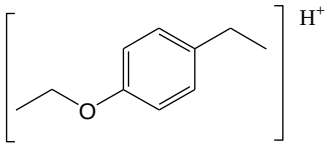
134.0	$[M+H-CH_3CH_2CH_2NH_2]^+$	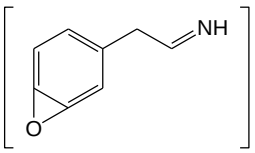

TP 194

m/z	Retention time	Precursor/ Product ion	Structure	References
194.1	12.0	$[M+H]^+$	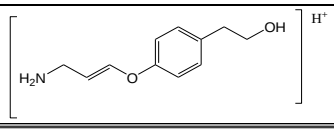	[27] MetaPC software

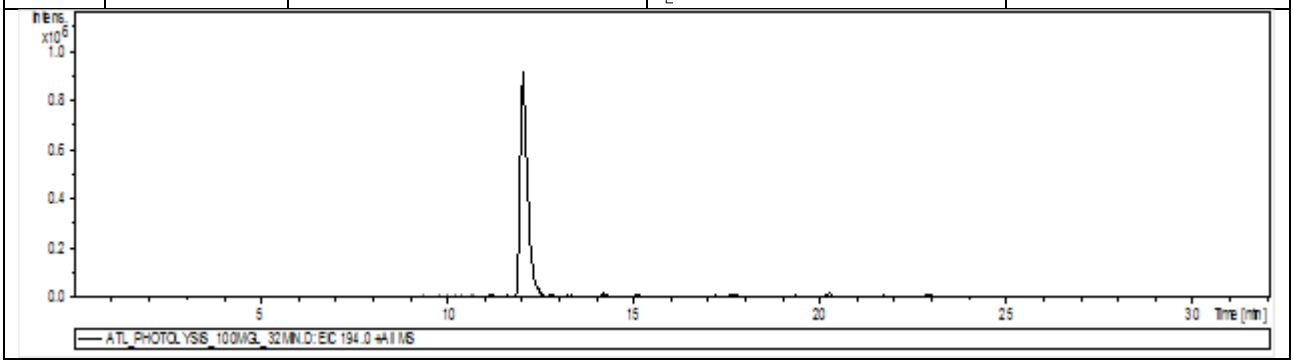

MS^2		
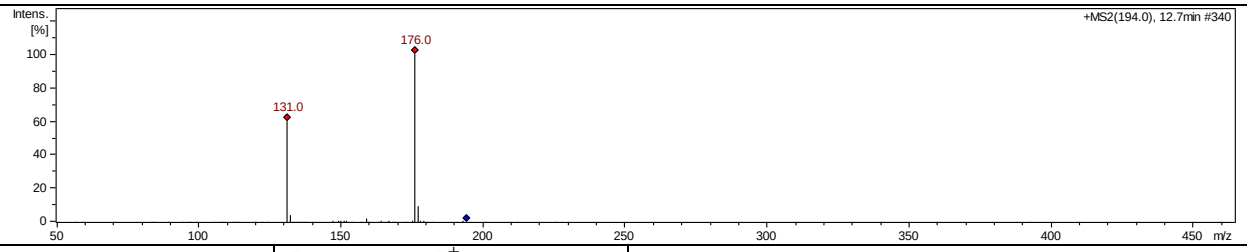		
176.0	$[M+H-H_2O]^+$	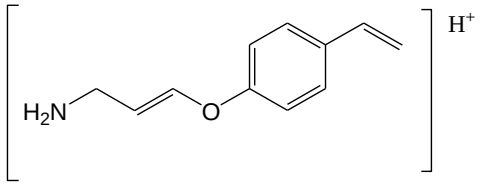
131.0	$[M+H-CH_3OH-CH_3NH_2]^+$	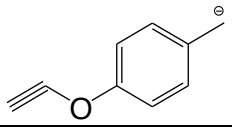

TP 207

m/z	Retention time	Precursor/ Product ion	Structure	References
207.1	9.2	$[M+H]^+$	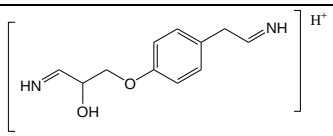	

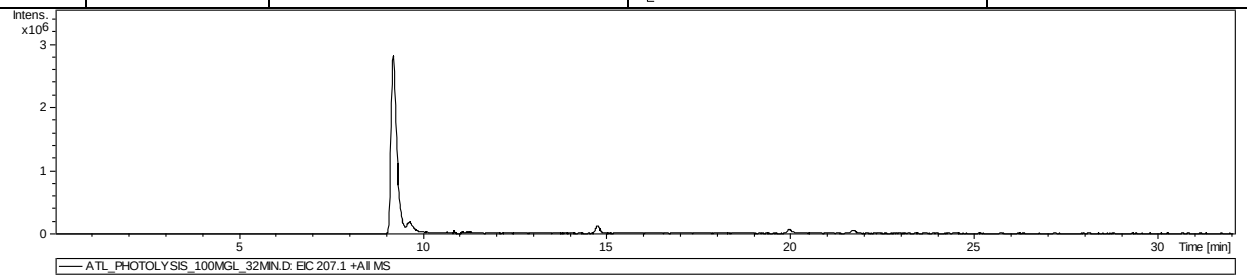

MS^2		
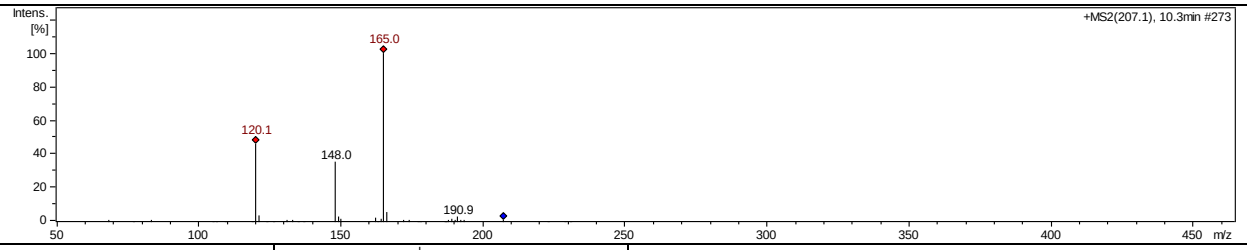		
190.9	$[M+H-O]^+$	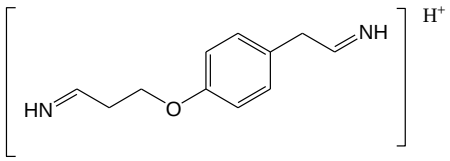
165.0	$[M+H-O-2NH_3]^+$	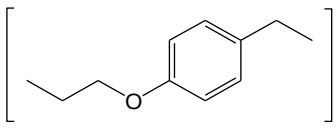

148.0	$[M+H-CH_2NH-CH_3OH]^+$	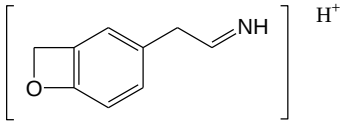
120.1	$[M+H-C_3H_7NO_2]^+$	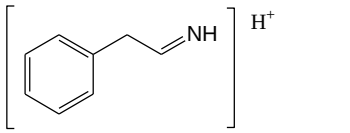

TP 210

m/z	Retention time	Precursor/ Product ion	Structure	References
210.0	14.6	$[M+H]^+$	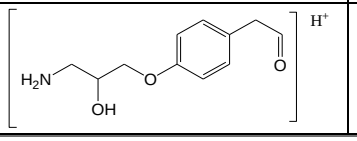	27

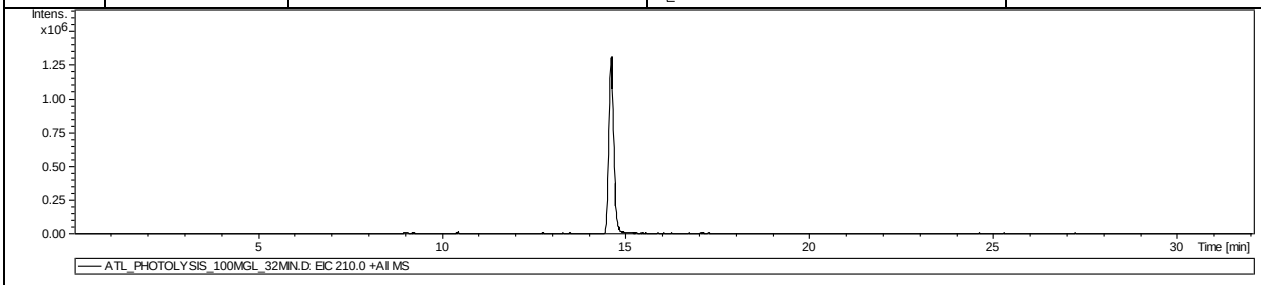

MS^2

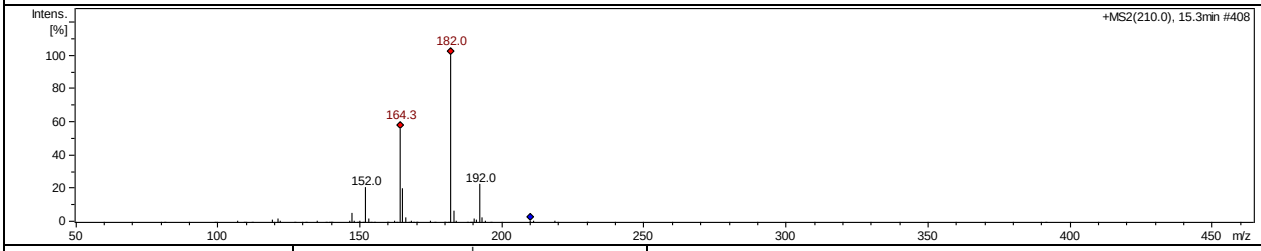

192.0	$[M+H-H_2O]^+$	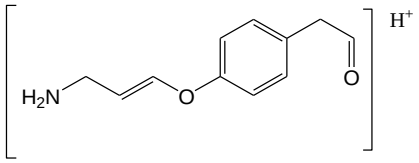
182.0	$[M+H-HCHO]^+$	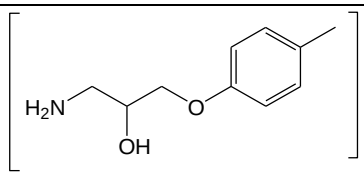
164.3	$[M+H-H_2O-HCHO]^+$	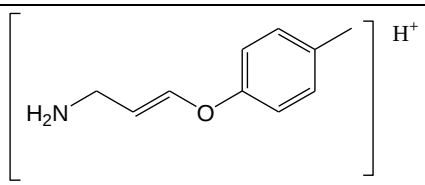

152.0	$[M+H-O-CH_3CHO]^+$	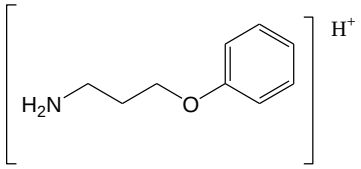

TP 223

m/z	Retention time	Precursor/ Product ion	Structure	References
223.1	10.7	$[M+H]^+$	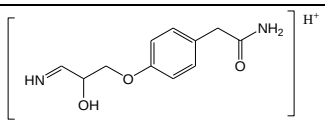	MetaPC software

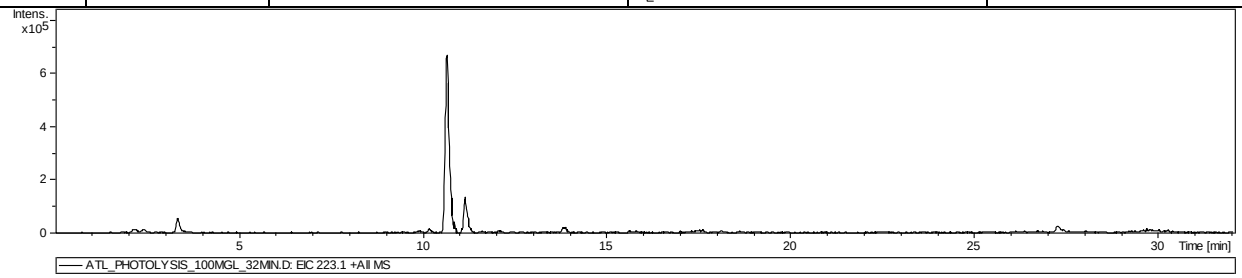

MS^2

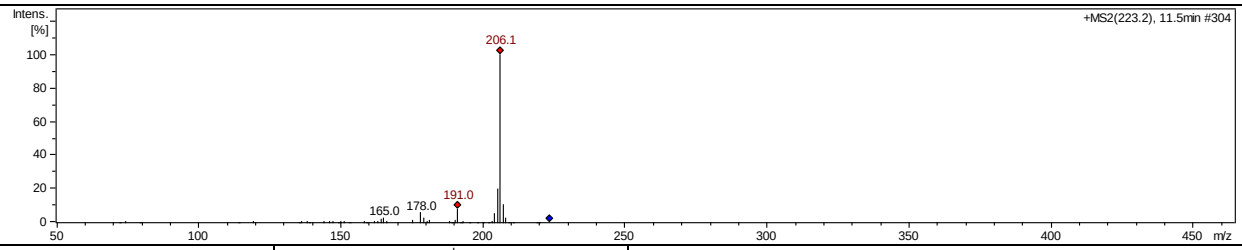

206.1	$[M+H-NH_3]^+$	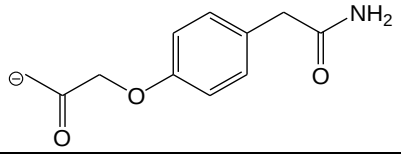
191.0	$[M+H-H_2O-O]^+$	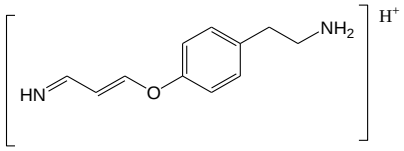
178.0	$[M+H-CH_3NH_2-H_2O]^+$	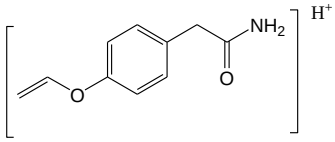
165.0	$[M+H-CH_2NH-H_2O-NH_3]^+$	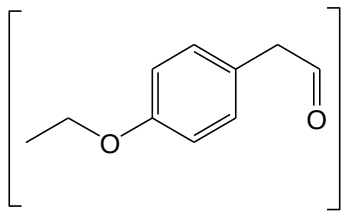

TP 225

m/z	Retention time	Precursor/ Product ion	Structure	References
225.1	5.5 min	$[M+H]^+$	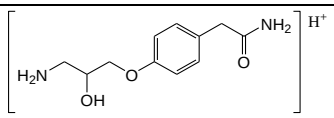	24,27 MetaPC software

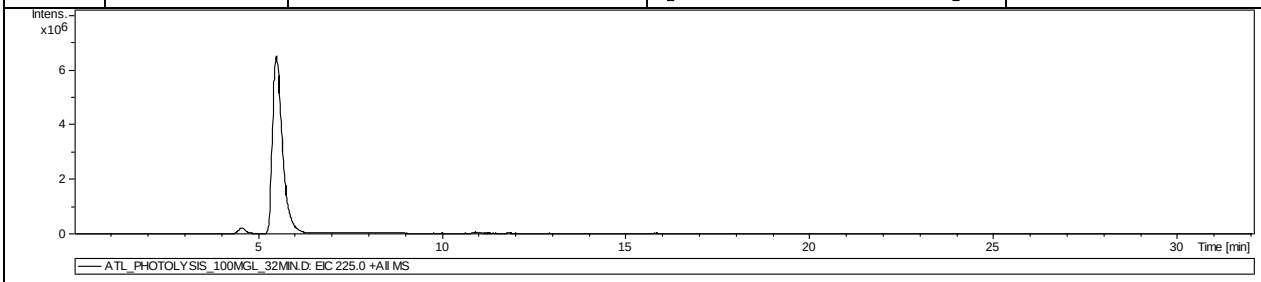

MS^2

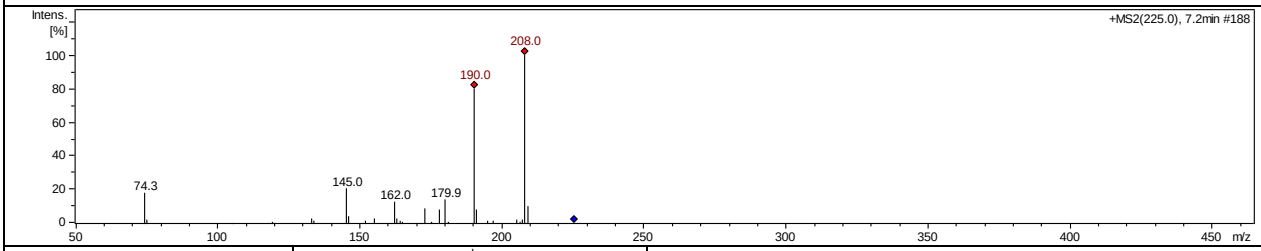

208.0	$[M+H-NH_3]^+$	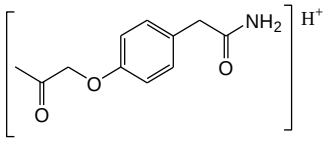
190.0	$[M+H-NH_3 – H_2O]^+$	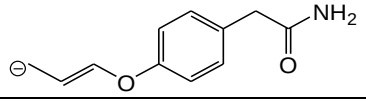
180.0	$[M+H-CHONH_2]^+$	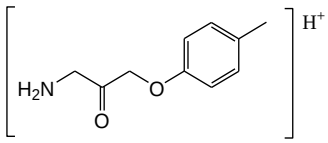
162.1	$[M+H-CHONH_2 – H_2O]^+$	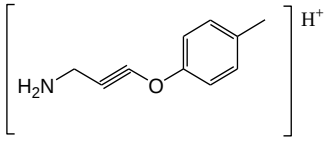
144.9	$[M+H-CHONH_2 – H_2O-NH_3]^+$	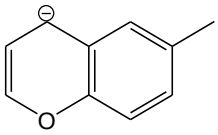
74.3	$[M+H-HOC_6H_4CH_2CONH_2]^+$	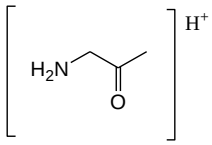

TP 232

m/z	Retention time	Precursor/ Product ion	Structure	References
232.1	13.2	$[M+H]^+$	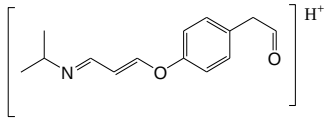	

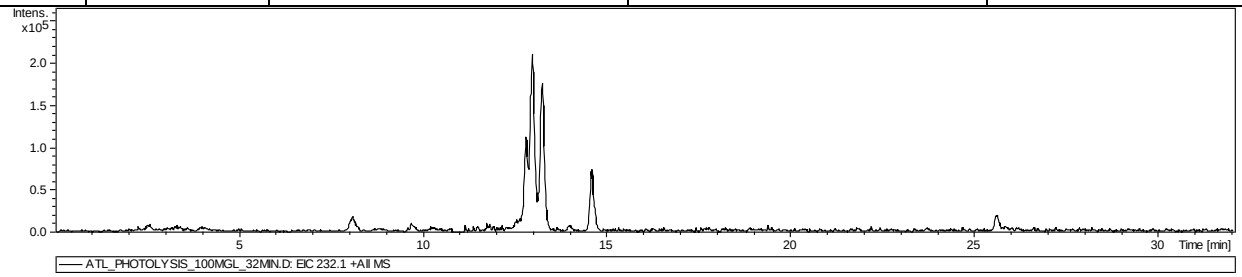

MS^2

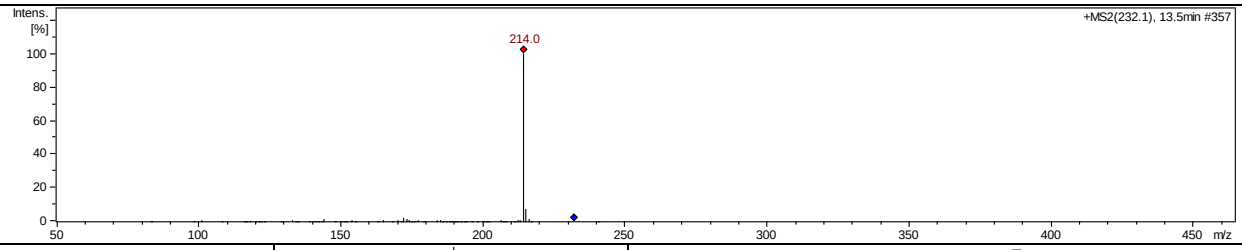

214.0	$[M+H-H_2O]^+$	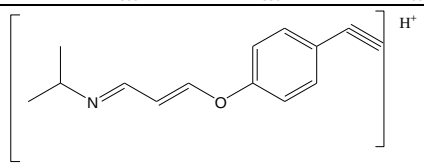

TP 238

m/z	Retention time	Precursor/ Product ion	Structure	References
238.1	12.9 min	$[M+H]^+$	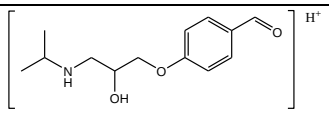	24,26 21

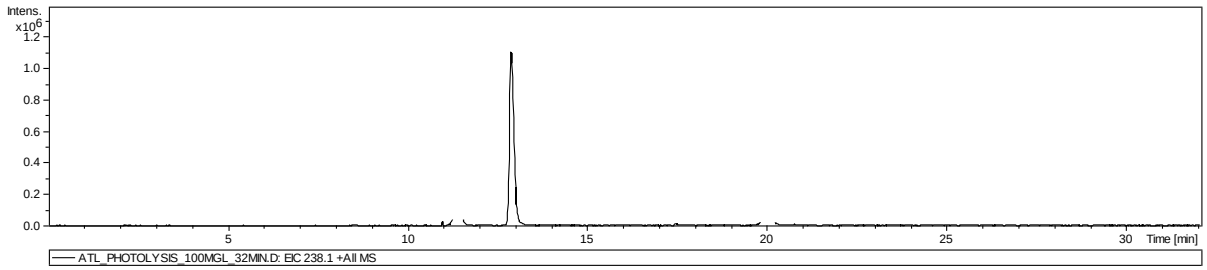

MS^2 of TP 238

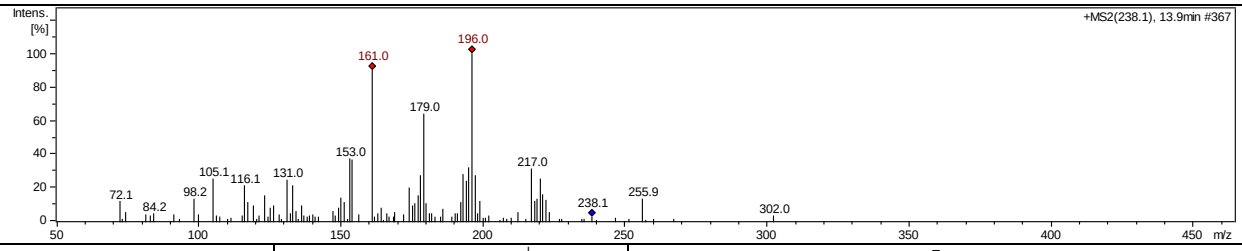

196.0	$[M+H-CH(CH_3)_2]^+$	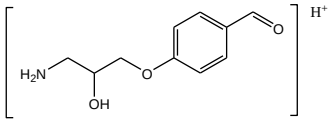
179.0	$[M+H- CH(CH_3)_2NH_2]^+$	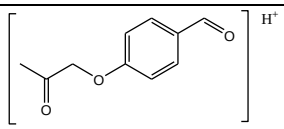
161.0	$[M+H- CH(CH_3)_2NH_2-H_2O]^+$	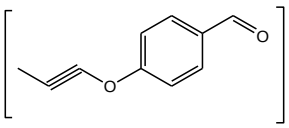
153.0	$[M+H- CH(CH_3)_2NH_2-HCHO]^+$	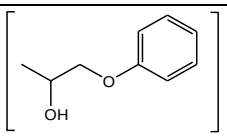
131.0	$[M+H- CH(CH_3)_2NH_2-H_2O-HCHO]^+$	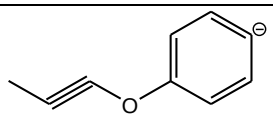
116.1	$[M+H-HOC_6H_4CHO]$	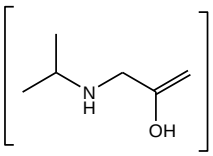
105.0	$[M+H-H_2OC_2H_6-CH_2NHCH(CH_3)_2-OH]^+$	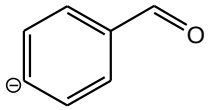

TP 249

m/z	Retention time	Precursor/ Product ion	Structure	References
249.1	14.0	$[M+H]^+$	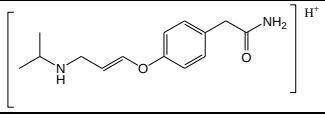	19 MetaPC software

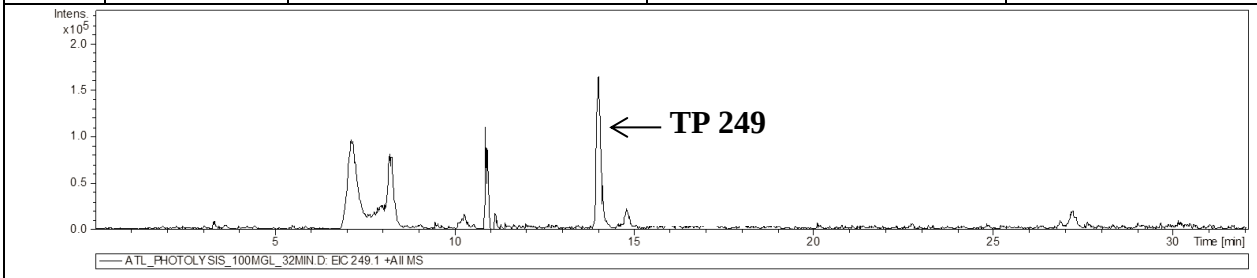

MS^2

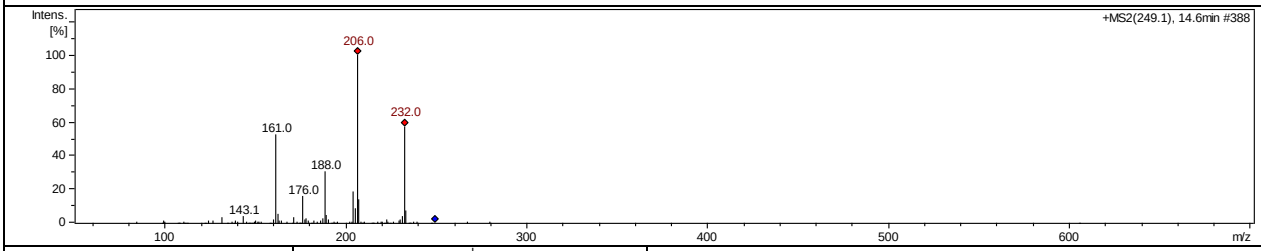

232.0	$[M+H-NH_3]^+$	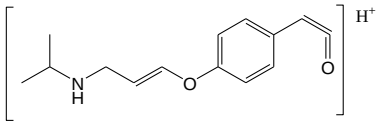
206.0	$[M+H-HCONH2]^+$	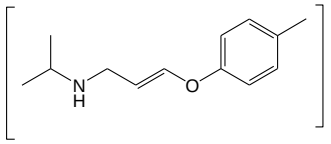
188.0	$[M+H-CH(CH_3)_2-NH_2]^+$	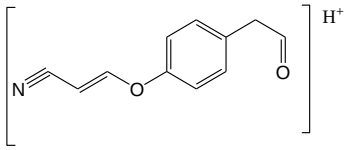
176.0	$[M+H-CH_3NHCH(CH_3)_2]^+$	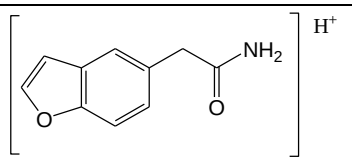
161.0	$[M+H-NHCH(CH_3)_2-NH_3-H_2O]^+$	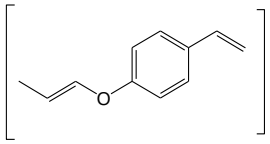

TP 253

m/z	Retention time	Precursor/ Product ion	Structure	References
253.1	13.1	$[M+H]^+$	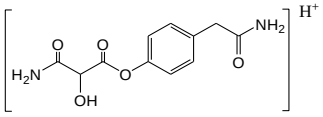	

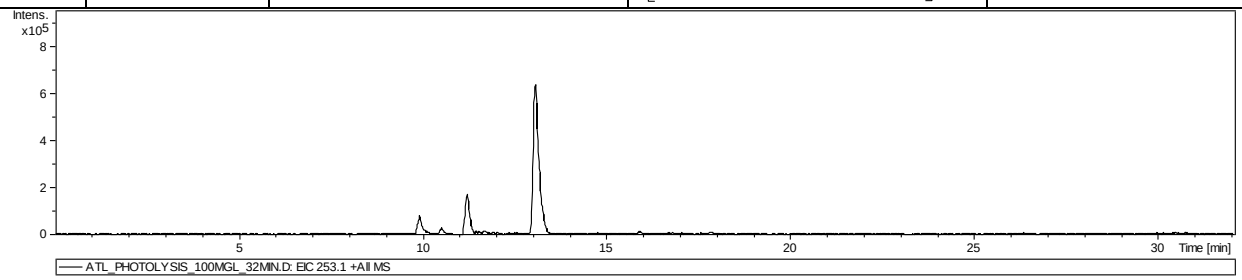

MS^2

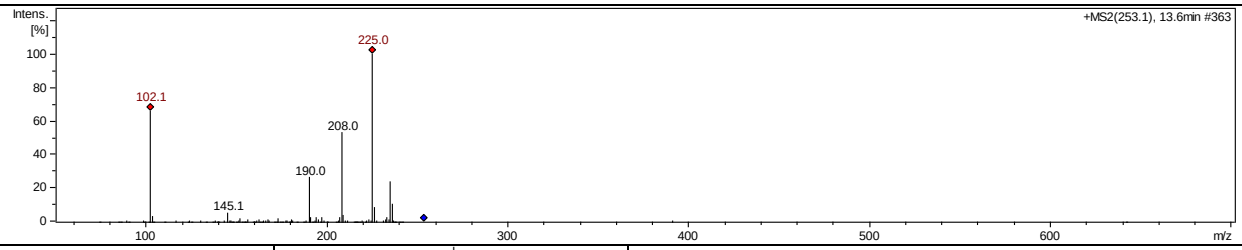

235.0	$[M+H-H_2O]^+$	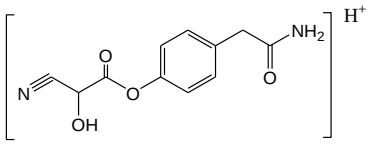
225.0	$[M+H-2O]^+$	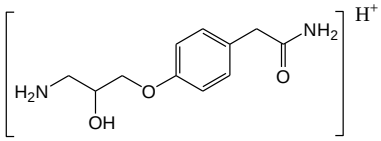
208.0	$[M+H-2O-NH_3]^+$	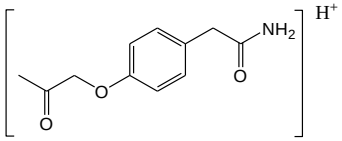
190.0	$[M+H-2O-NH_3-H_2O]^+$	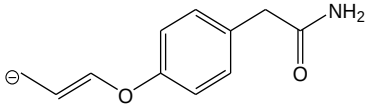
142.1	$[M+H-2O-NH_3-H_2O-HCONH_2]^+$	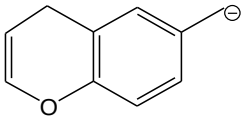
102.1	$[M+H-C_8H_9NO_2]^+$	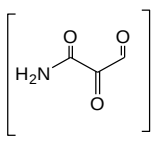

TP 254

m/z	Retention time	Precursor/ Product ion	Structure	References
254.1	12.3	$[M+H]^+$	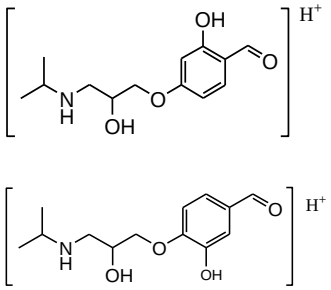	26 20,21,28

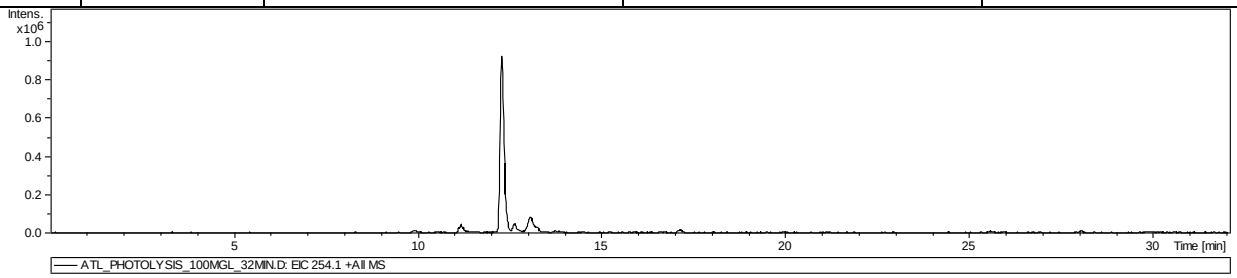

MS^2

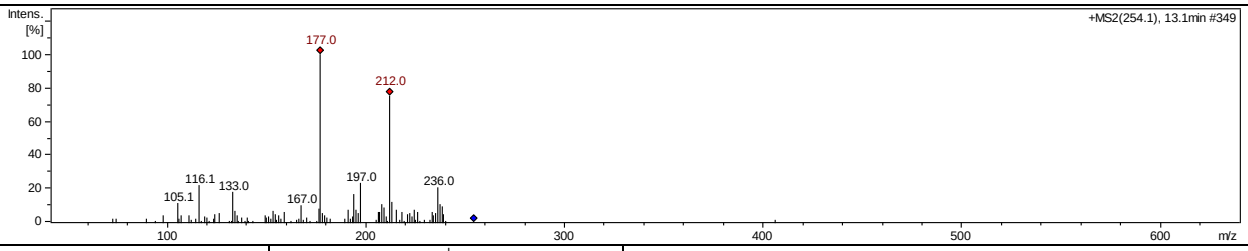

236.0	$[M+H-H_2O]^+$	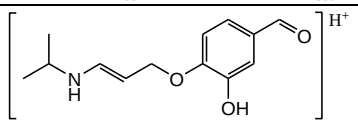
212.0	$[M+H-CH(CH_3)_2]^+$	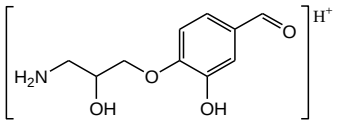
197.0	$[M+H-NHCH(CH_3)_2]^+$	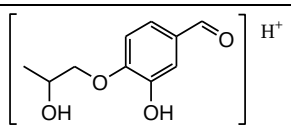
194.0	$[M+H-H_2O-CH(CH_3)_2]^+$	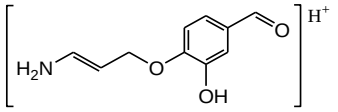
177.0	$[M+H-NH2CH(CH_3)_2-H_2O]^+$	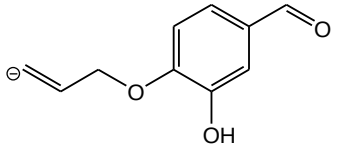
133.0	$[M+H-NH2CH(CH_3)_2-H_2O-HCHO-O]^+$	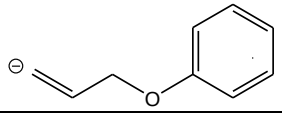

116.1	$[M+H-C_7H_6O_3]^+$	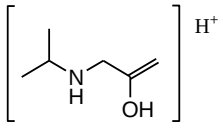
105.1	$[M+H-C_5H_{13}NO-H_2O-HCHO]^+$	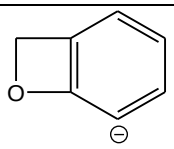

TP 265

m/z	Retention time	Precursor/ Product ion	Structure	References
265.1	9.4	$[M+H]^+$	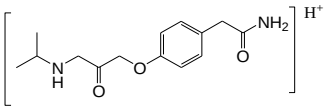	MetaPC software

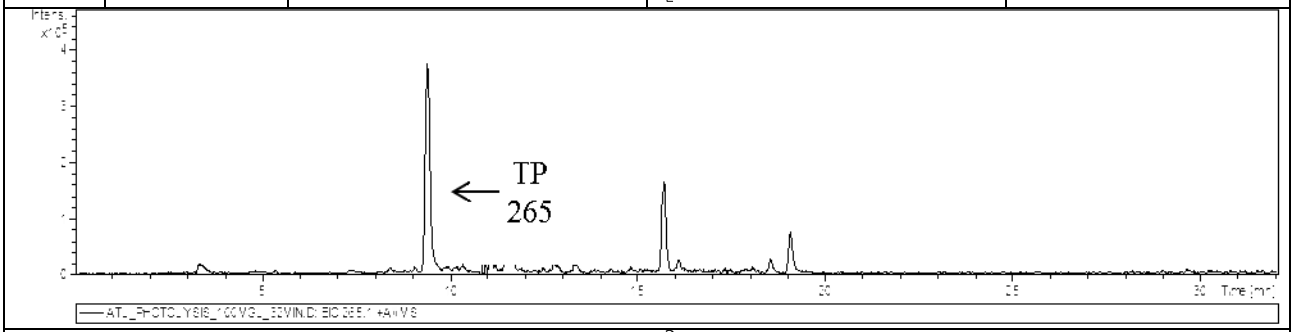

MS^2

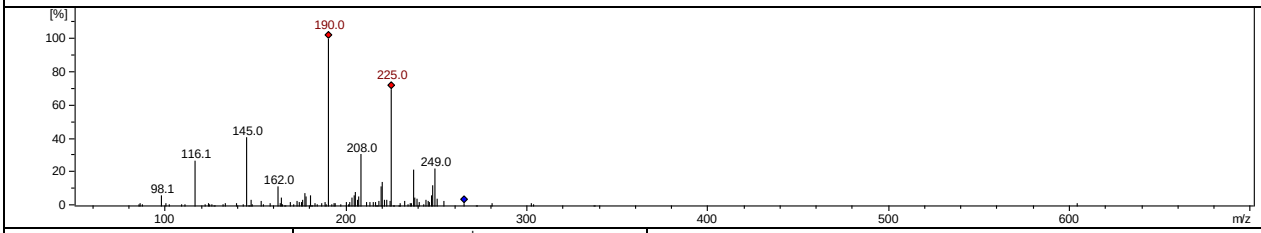

249.0	$[M+H-H_2O]^+$	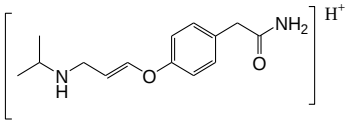
237.0	$[M+H-2O]^+$	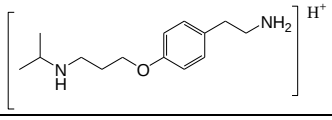
225.0	$[M+H-CH(CH_3)_2]^+$	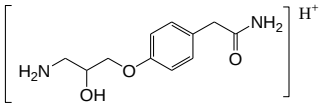
208.0	$[M+H-CHNH(CH_3)_2]^+$	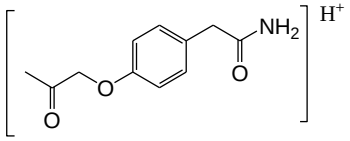
190.0	$[M+H-H_2O-CH_3CONH_2]^+$	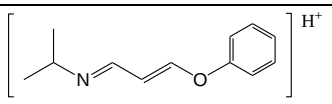

162.0	$[M+H-2H_2O-CH_3NHCH(CH_3)_2]^+$	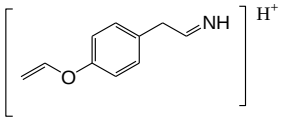
145.0	$[M+H-2H_2O-CH_3NHCH(CH_3)_2-NH_3]^+$	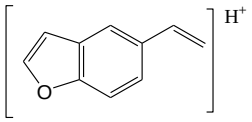
116.1	$[M+H-C_8H_9NO_2]^+$	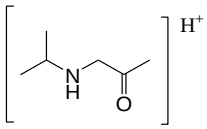
98.1	$[M+H-C_8H_9NO_2-H_2O]^+$	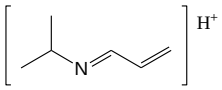

TP 275

m/z	Retention time	Precursor/ Product ion	Structure	References
275.2	2.0 min	$[M+H]^+$	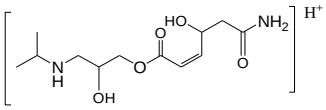	

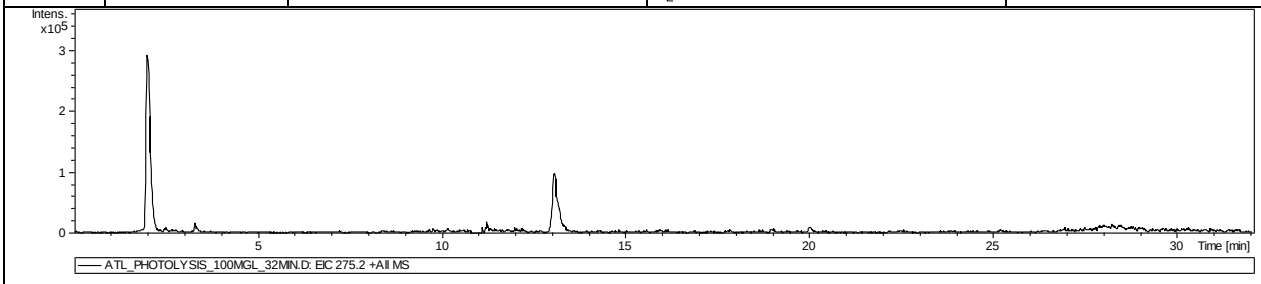

MS^2

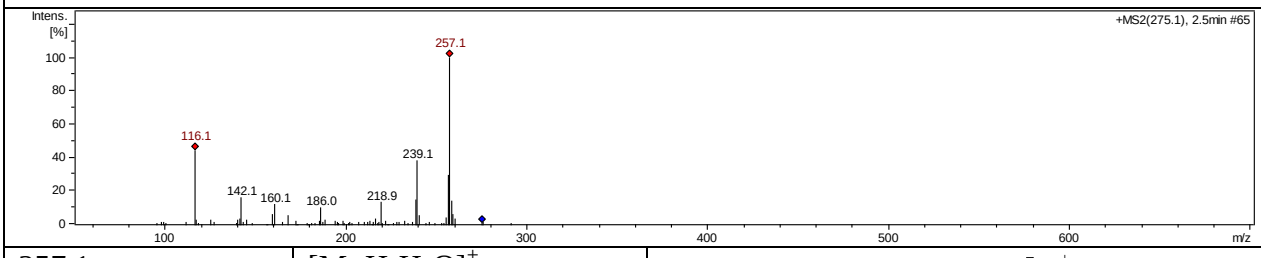

257.1	$[M+H-H_2O]^+$	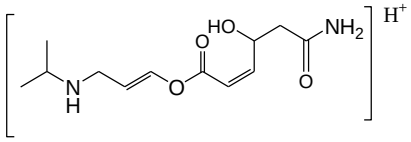
239.1	$[M+H-2H_2O]^+$	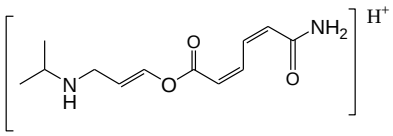
186.0	$[M+H-H_2O-NHCH(CH_3)_2-O]^+$	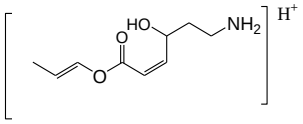

142.1	$[M+H-C_6H_{15}NO_2]^+$	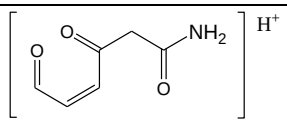
116.1	$[M+H-C_6H_9NO_4]^+$	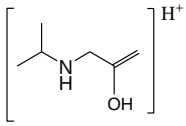

TP 281

m/z	Retention time	Precursor/ Product ion	Structure	References
281.2	several peaks	$[M+H]^+$	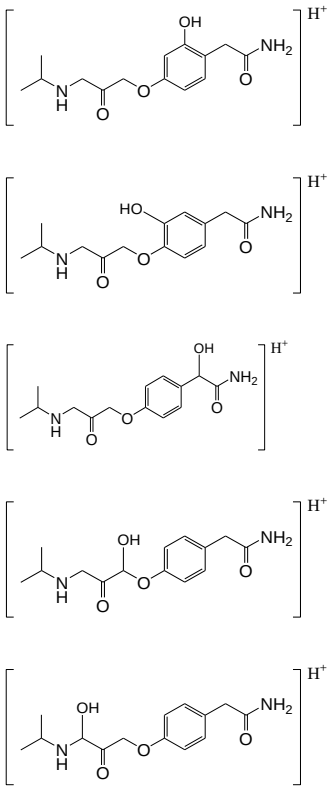	20,21,24 MetaPC software

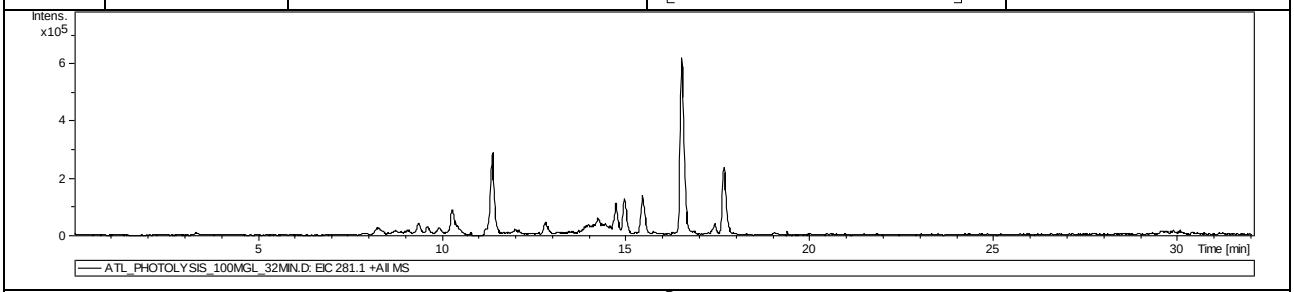

MS^2

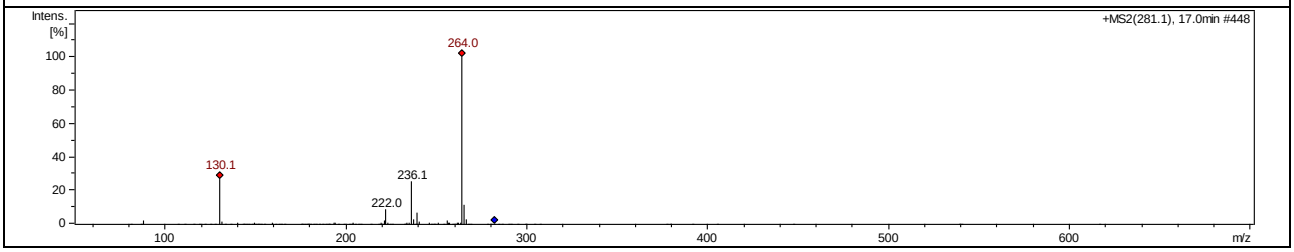

264.0	$[M+H-NH_3]^+$	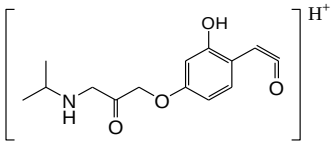
239.0	$[M+H-CH(CH_3)_2]^+$	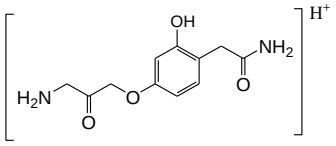
236.1	$[M+H-HCONH_2]^+$	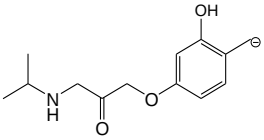
222.0	$[M+H-NH_2CH(CH_3)_2]^+$	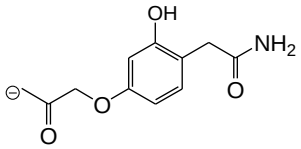
130.1	$[M+H-C_8H_9NO_2]^+$	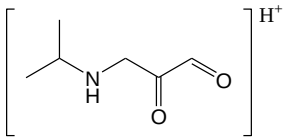

TP 283

m/z	Retention time	Precursor/ Product ion	Structure	References
283.2	several peaks	$[M+H]^+$	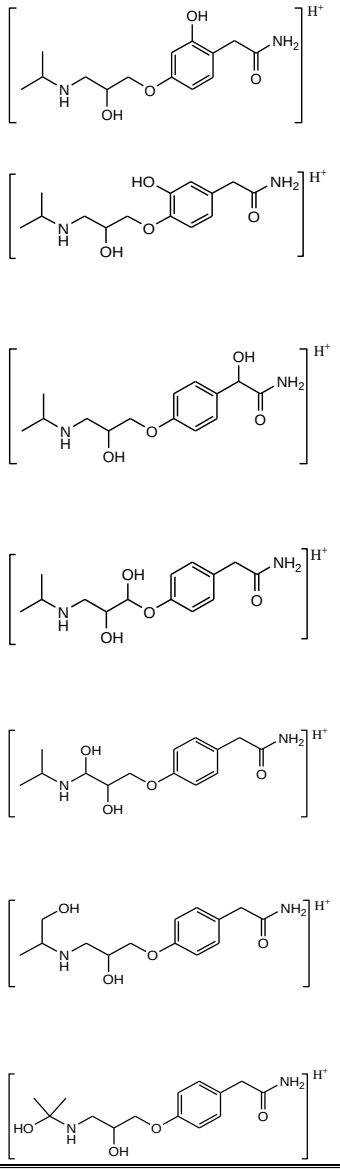	20–22,24,26–28 MetaPC software

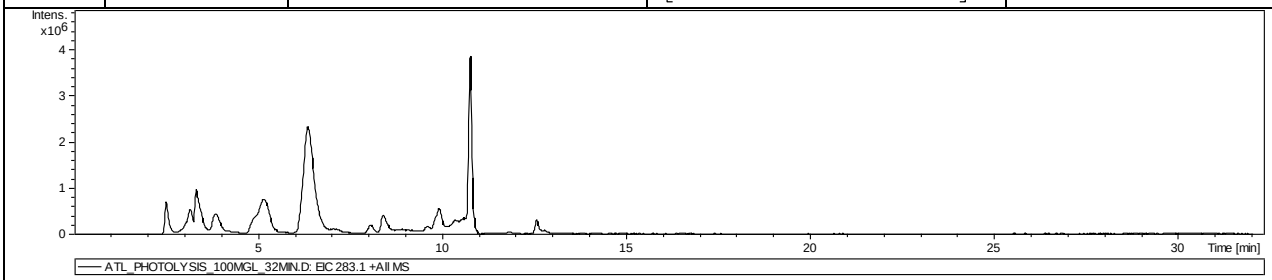

MS^2

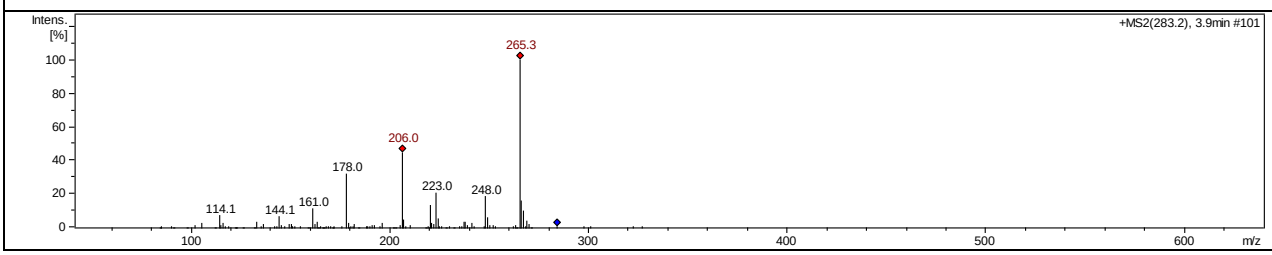

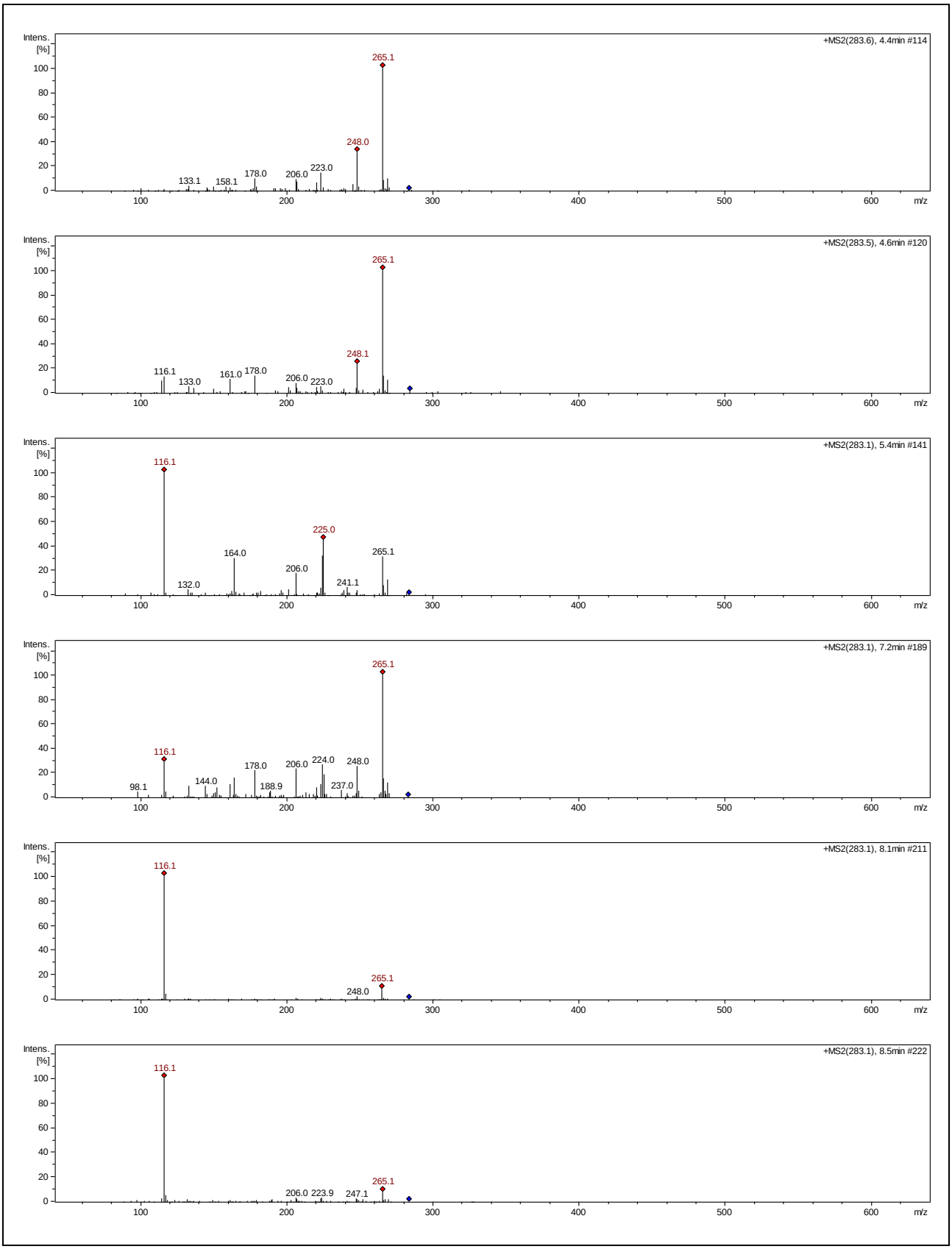
Intens.
[%]
+MS2(283.6), 4.4min #114
265.1
248.0
133.1
158.1
178.0
206.0
223.0
+MS2(283.5), 4.6min #120
265.1
248.1
116.1
133.0
161.0
178.0
206.0
223.0
+MS2(283.1), 5.4min #141
116.1
225.0
164.0
265.1
206.0
132.0
241.1
+MS2(283.1), 7.2min #189
265.1
116.1
178.0
206.0
224.0
248.0
98.1
144.0
188.9
237.0
+MS2(283.1), 8.1min #211
116.1
265.1
248.0
+MS2(283.1), 8.5min #222
116.1
265.1
206.0
223.9
247.1
m/z

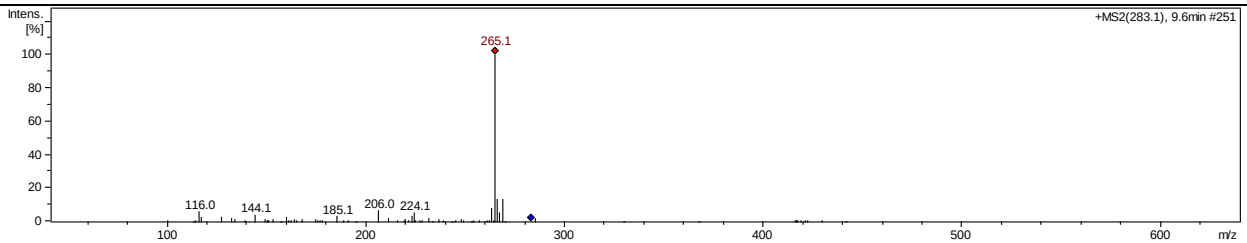

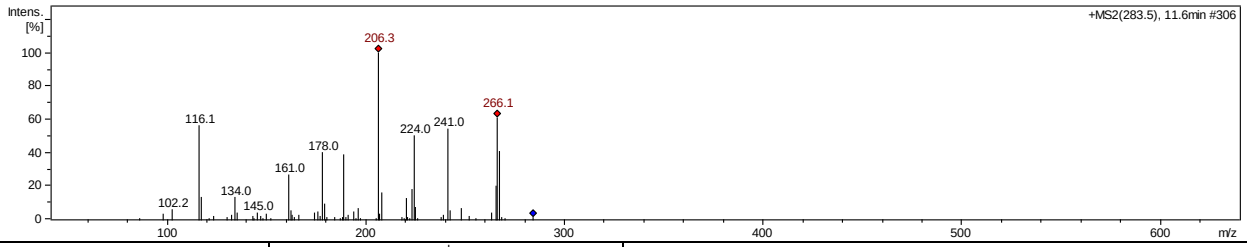

265.1	$[M+H-H_2O]^+$	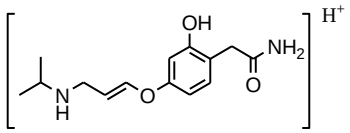
248.0	$[M+H-H_2O-NH_3]^+$	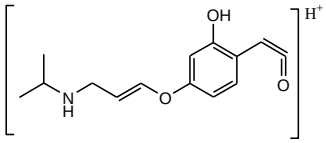
241.1	$[M+H-CH(CH_3)_2]^+$	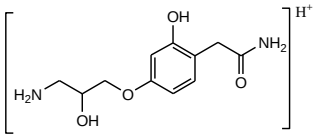
225.0	$[M+H-CH(CH_3)_2-O]^+$	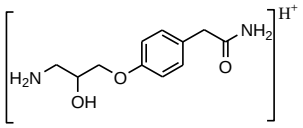
223.0	$[M+H-CH(CH_3)_2-H_2O]^+$	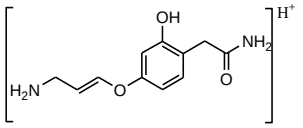
220.0	$[M+H-CH2(CH_3)_2-NH_3]^+$	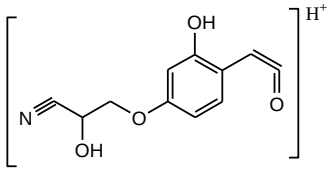
206.0	$[M+H-CH(CH_3)_2-H_2O-NH_3]^+$	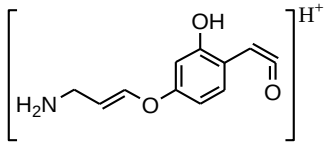
190.0	$[M+H-NH_2CH(CH_3)_2-H_2O-O]^+$	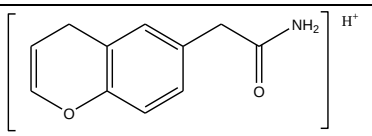
178.0	$[M+H-CH_3NHCH(CH_3)_2-H_2O-O]^+$	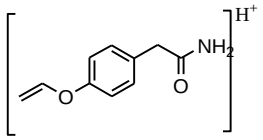

161.0	[M+H-$CH_3NHCH(CH_3)_2$-H_2O-O-NH_3]$^+$	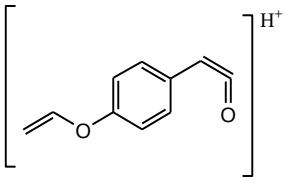
144.0	[M+H-CH2$(CH_3)_2$-H_2O-O-CH_3CONH_2]$^+$	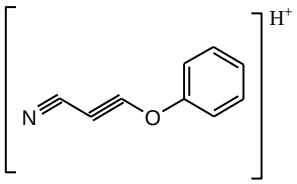
132.0	[M+H-$C_8H_{11}NO_2$]$^+$	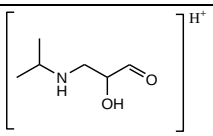
116.1	[M+H-$C_8H_{11}NO_3$]$^+$	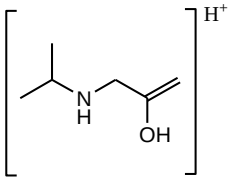
98.2	[M+H-$C_8H_{11}NO_3$-H_2O]$^+$	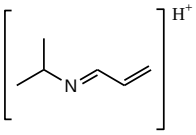

TP 285

m/z	Retention time	Precursor/ Product ion	Structure	References
285.3	13.8	[M+H]$^+$	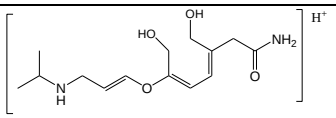	

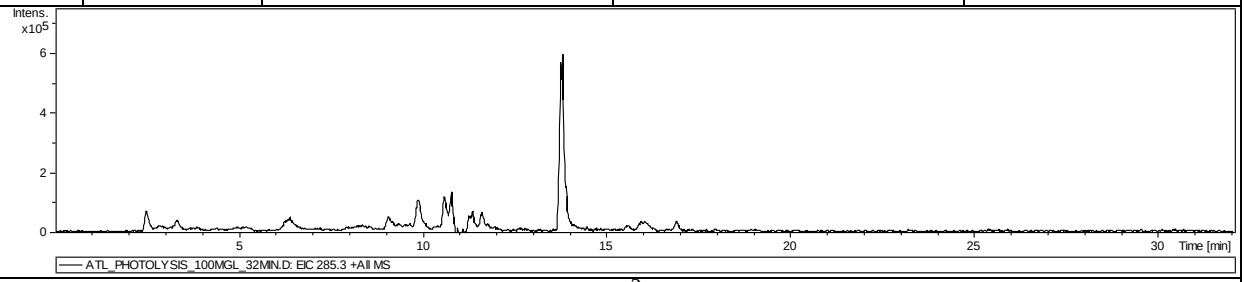

MS^2

NO MS2 fragment observed

TP 287

m/z	Retention time	Precursor/ Product ion	Structure	References

287.3	14.8 min	$[M+H]^+$	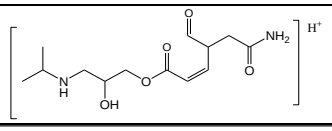	

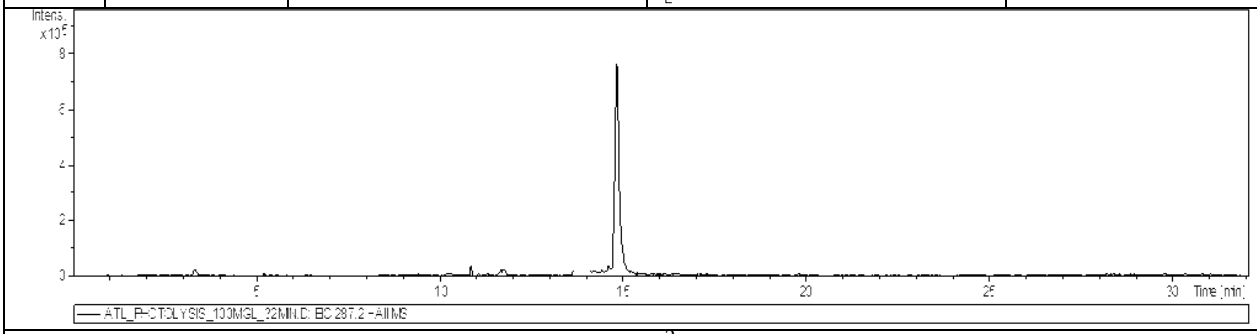

MS^2

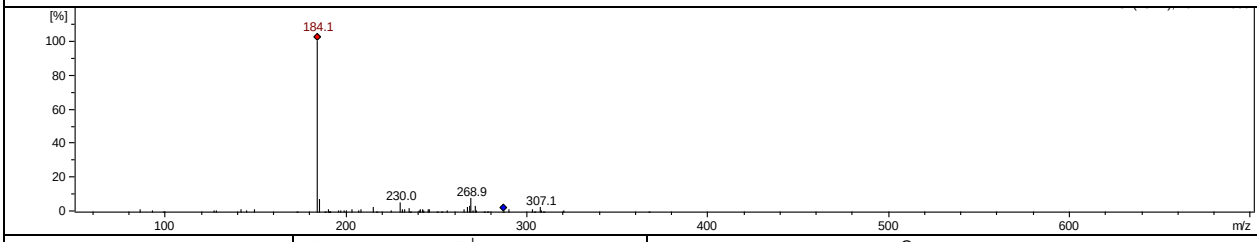

268.9	$[M+H-H_2O]^+$	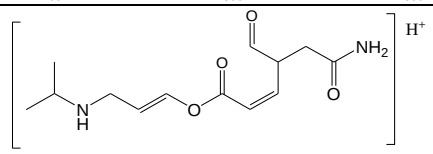
230.0	$[M+H-NH_2CH(CH_3)_2]^+$	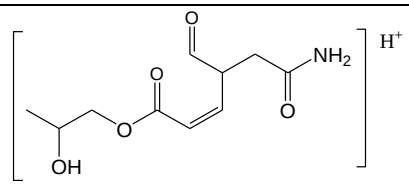
184.1	$[M+H-NH_2CH(CH_3)_2-H2O-HCHO]^+$	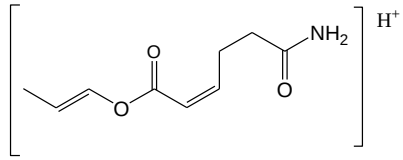

TP 295

m/z	Retention time	Precursor/ Product ion	Structure	References
295.2	12.6 min 17.6 min	$[M+H]^+$	TP_1 295 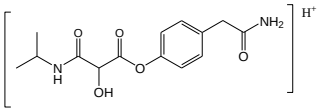 TP_2 295 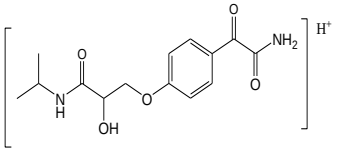	29

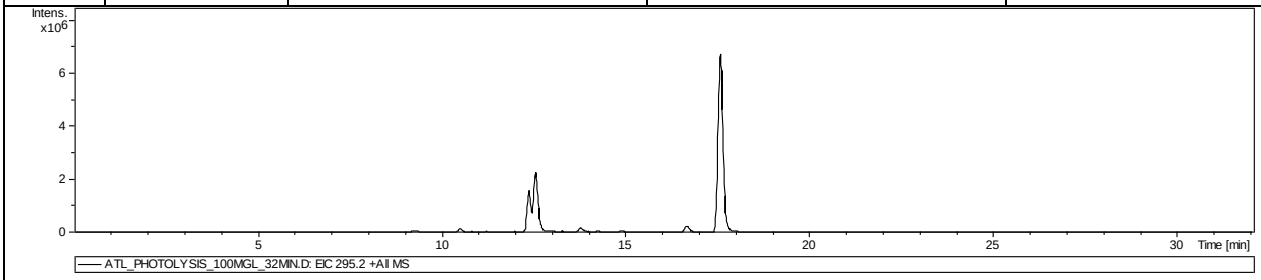

MS^2 of TP_1 295

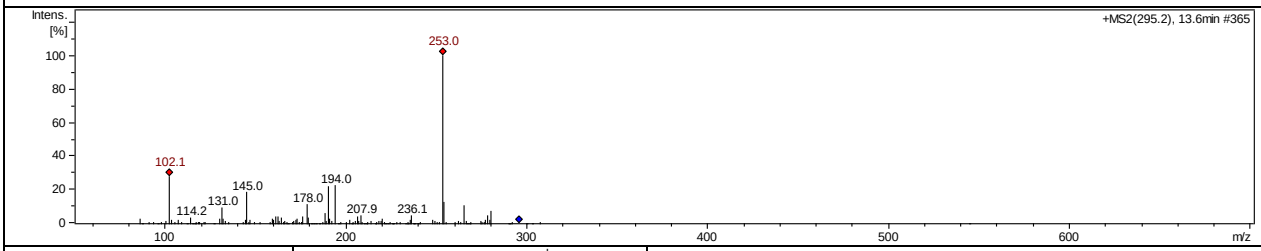

253.0	$[M+H-CH(CH_3)_2]^+$	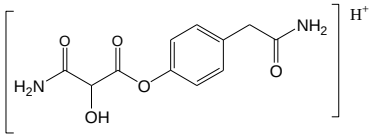
194.0	$[M+H-2H_2O-NHCH(CH_3)_2]^+$	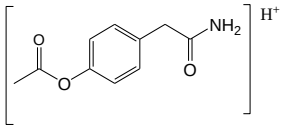
190.0	$[M+H-2H_2O-NHCH(CH_3)_2-H_2O]^+$	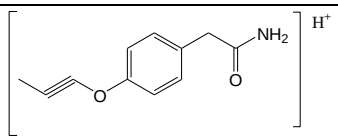
145.0	$[M+H-2H_2O-NHCH(CH_3)_2-H_2O-HCONH_2]^+$	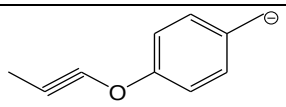
131.0	$[M+H-2H_2O-NHCH(CH_3)_2-H_2O-CH_3CONH_2]^+$	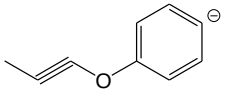

102.1	$[M+H-C_9H_{11}NO_3]^+$	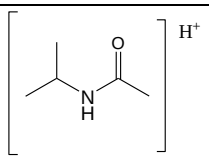
MS^2 of TP_2 295		
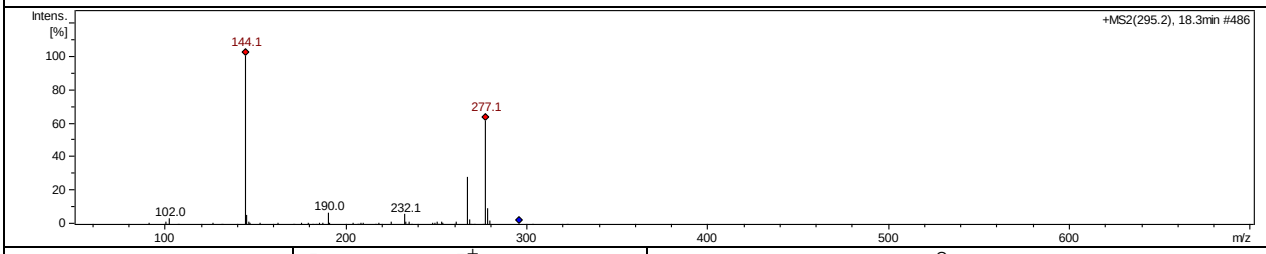		
277.1	$[M+H-H_2O]^+$	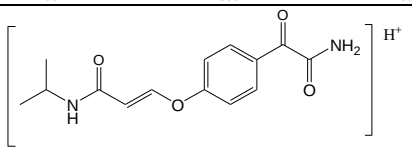
267.1	$[M+H-2O]^+$	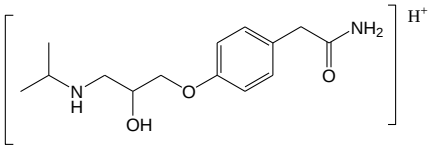
190.1	$[M+H-2H_2O-CH_3NHCH(CH_3)_2]^+$	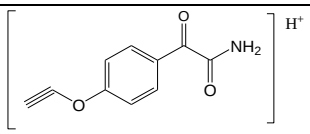
144.1	$[M+H-C_8H_9NO_2]^+$	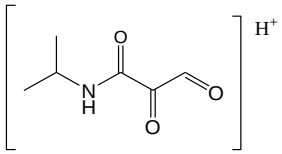
102.0	$[M+H-C_9H_{11}NO_4]^+$	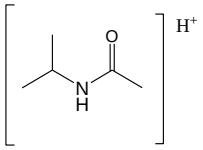

TP 297

m/z	Retention time	Precursor/ Product ion	Structure	References
297.1	14.1 min 17.6 min	$[M+H]^+$	TP_1 297 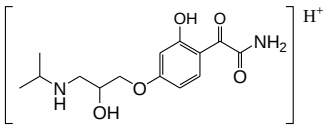 TP_2 297 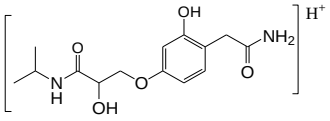	20

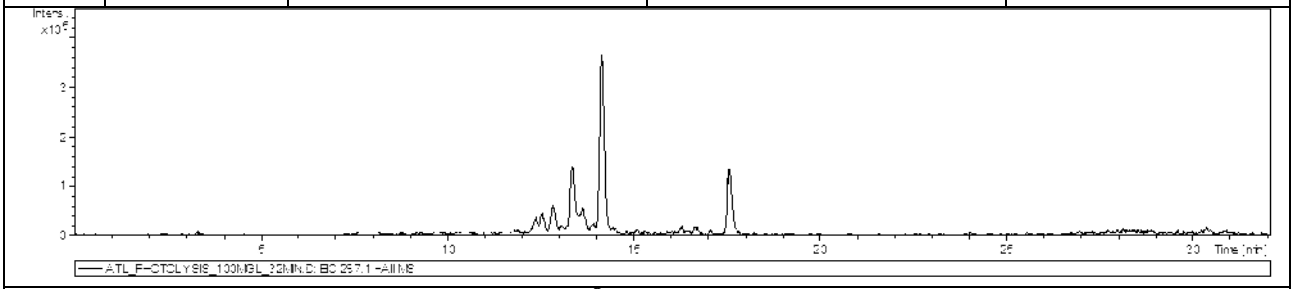

MS^2 of TP_1 297

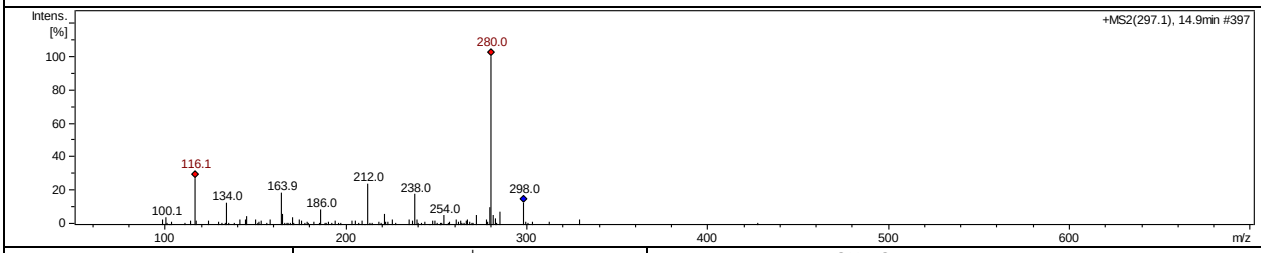

280.0	$[M+H-NH_3]^+$	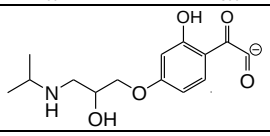
238.0	$[M+H-NH_2CH(CH_3)_2]^+$	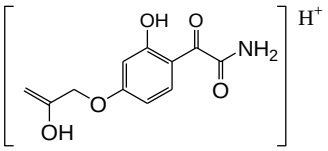
212.0	$[M+H-$ O-$CH_3NHCH(CH_3)_2]^+$	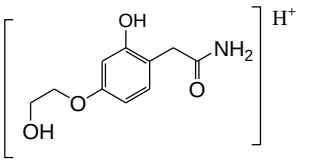
163.9	$[M+H-C_6H_{15}\ NO_2]^+$	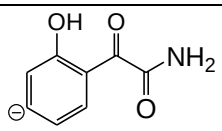
134.0	$[M+H-C_8H_7NO_3]^+$	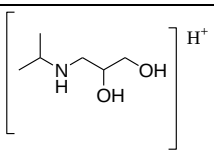

116.1	$[M+H-C_8H_7NO_3-H_2O]^+$	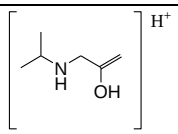
100.1	$[M+H-C_8H_7NO_3-2H_2O]^+$	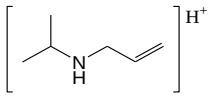
MS^2 of TP_2 297		
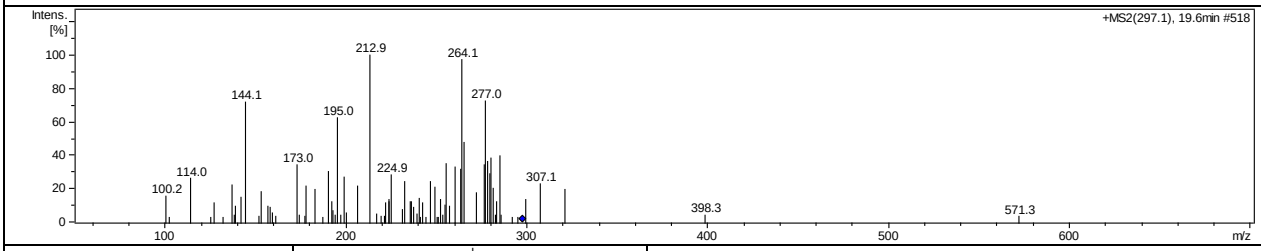		
280.2	$[M+H-NH_3]^+$	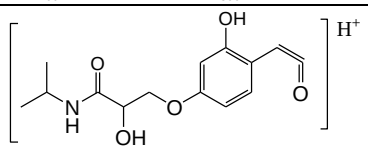
277.0	$[M+H-H_2O]^+$	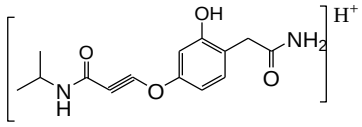
264.0	$[M+H-H_2O-NH_3]^+$	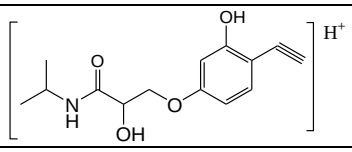
212.9	$[M+H-HCHO-NH_2CH(CH_3)_2]^+$	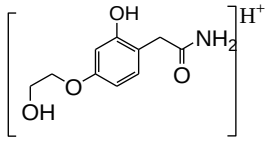
195.0	$[M+H-CH(CH_3)_2-H_2O-3O]^+$	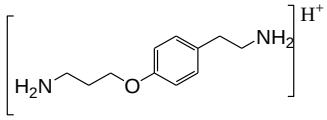
144.1	$[M+H-C_8H_{13}NO_2]^+$	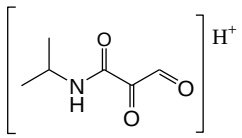
114.0	$[M+H-C_8H_{13}NO_2-H_2O-O]^+$	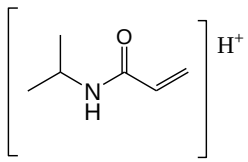

TP 299

m/z	Retention time	Precursor/ Product ion	Structure	References
299.1	3.3 min	$[M+H]^+$	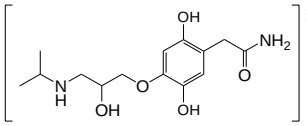	20,24,26

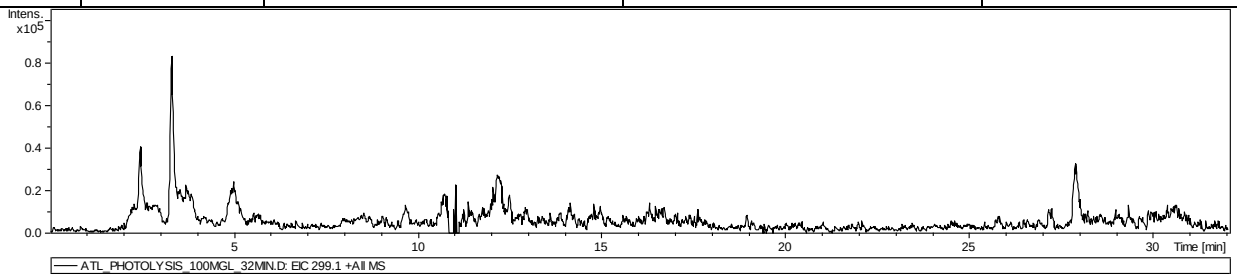

MS^2

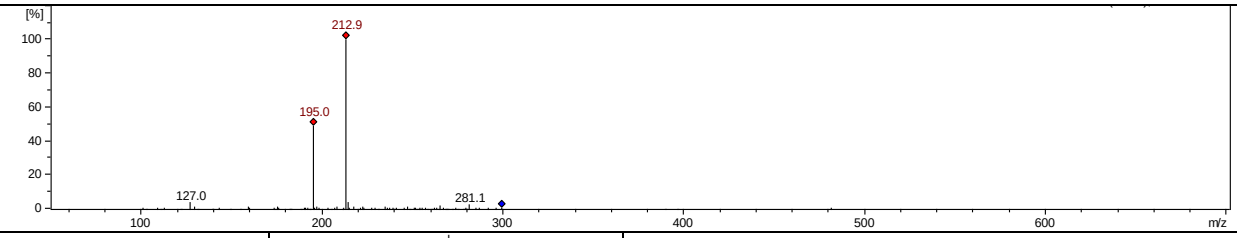

281.1	$[M+H-H_2O]^+$	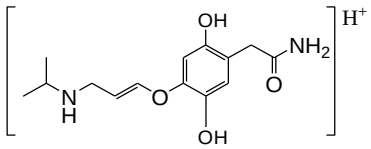
212.9	$[M+H-2H_2O-CH(CH_3)_2-O]^+$	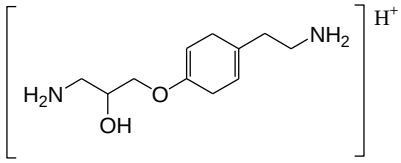
195.0	$[M+H-3H_2O-CH(CH_3)_2-O]^+$	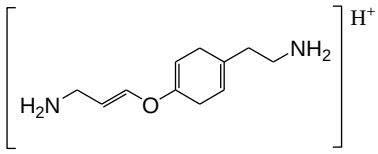

TP 301

m/z	Retention time	Precursor/ Product ion	Structure	References
301.2	several Peaks	$[M+H]^+$	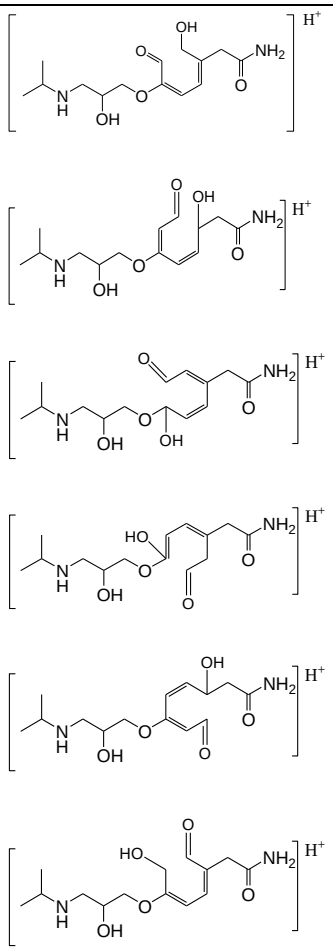	

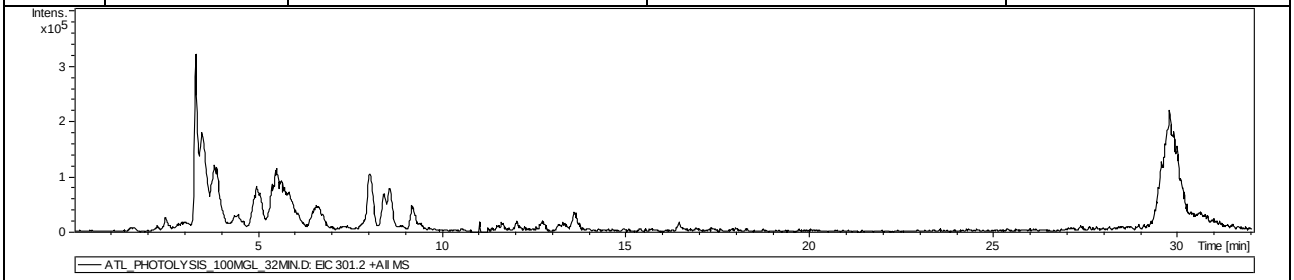

MS^2

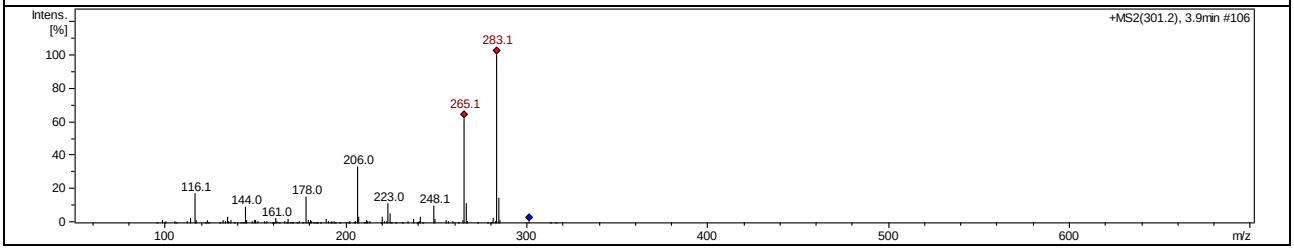

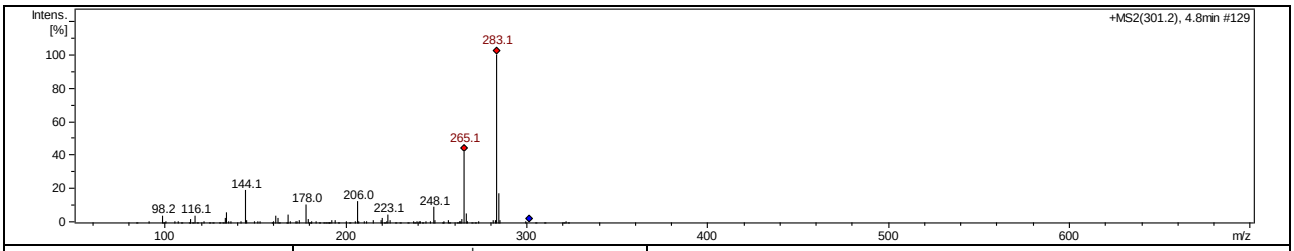

283.1	$[M+H-H_2O]^+$	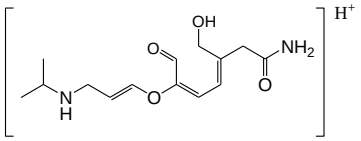
265.1	$[M+H-2H_2O]^+$	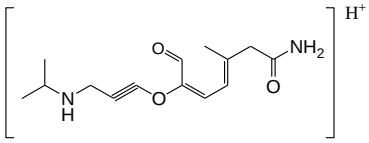
248.1	$[M+H-2H_2O-NH_3]^+$	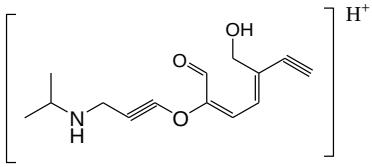
223.1	$[M+H-CH2(CH_3)_2-2H_2O]^+$	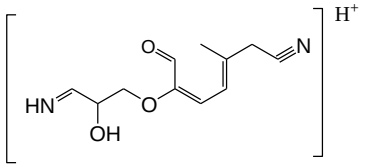
178.0	$[M+H-NH_2CH(CH_3)_2-2H_2O-CH_3OH]^+$	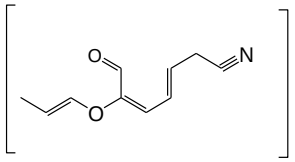
144.0	$[M+H-CH2(CH_3)_2-C_5H_9NO_2]^+$	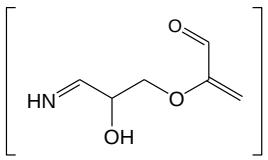
134.0	$[M+H-C_8H_{11}NO_3]^+$	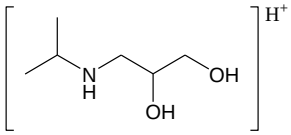
116.1	$[M+H-C_8H_{11}NO_3-H_2O]^+$	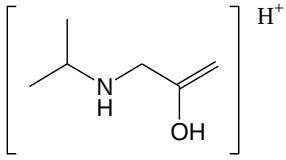

TP 309

m/z	Retention time	Precursor/ Product ion	Structure	References
309.2	TP_1 309 11.2 TP_2 309 14.2	$[M+H]^+$	TP_1 309 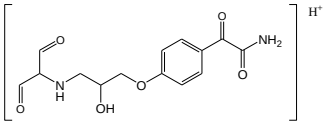 TP_2 309 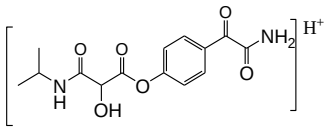	29
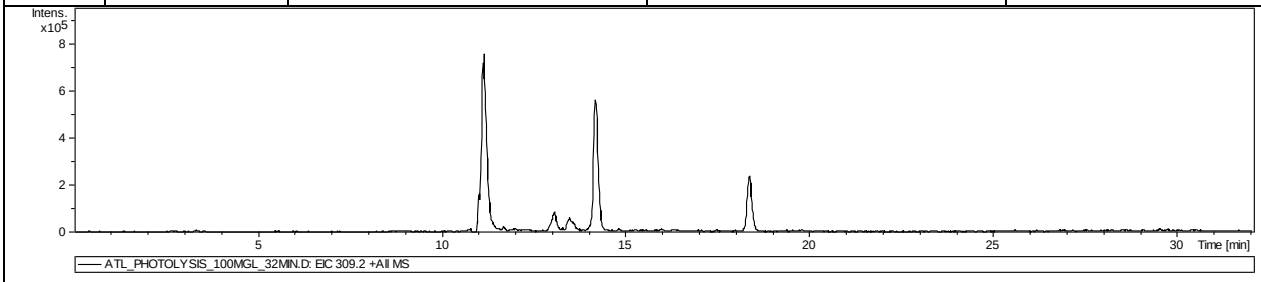				
MS^2 of TP_1 309				
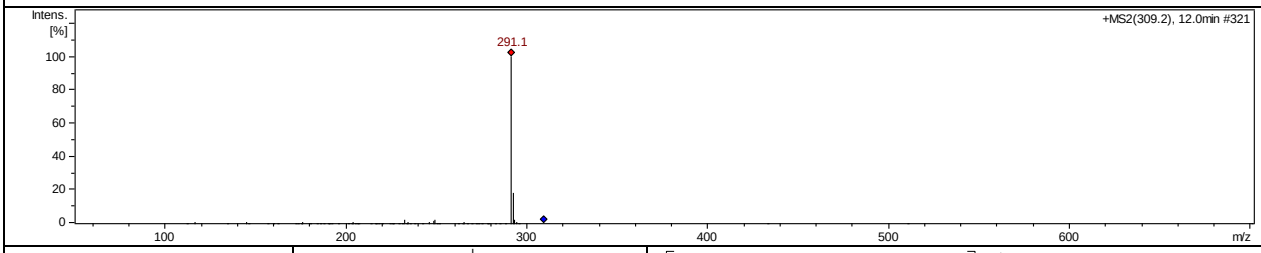				
291.1	$[M+H-H_2O]^+$		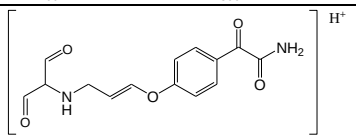	
MS^2 of TP_2 309				
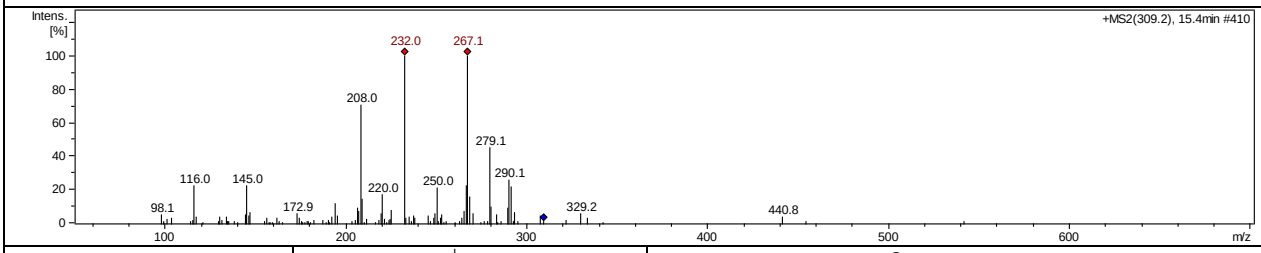				
279.1	$[M+H-2O]^+$		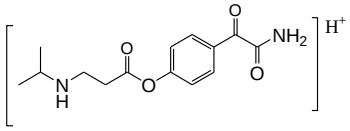	
267.1	$[M+H-CH_2(CH_3)_2]^+$		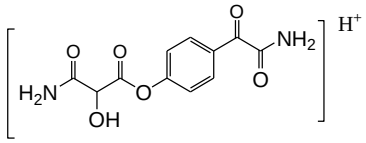	

232.0	$[M+H-H_2O-CH_2(CH_3)_2-NH_3]^+$	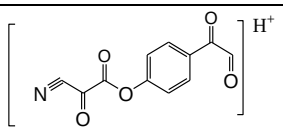
208.0	$[M+H-NH_2CH(CH_3)_2-HCHO-H_2O]^+$	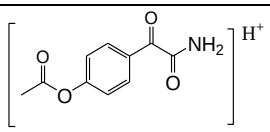
145.0	$[M+H-C_8H_7NO_3]^+$	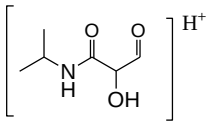
116.0	$[M+H-C_8H_7NO_3-HCHO]^+$	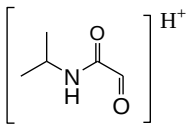

TP 310

m/z	Retention time	Precursor/ Product ion	Structure	References
310.2	17.3 min	$[M+H]^+$	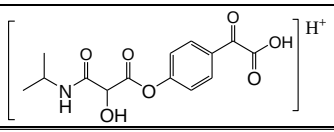	

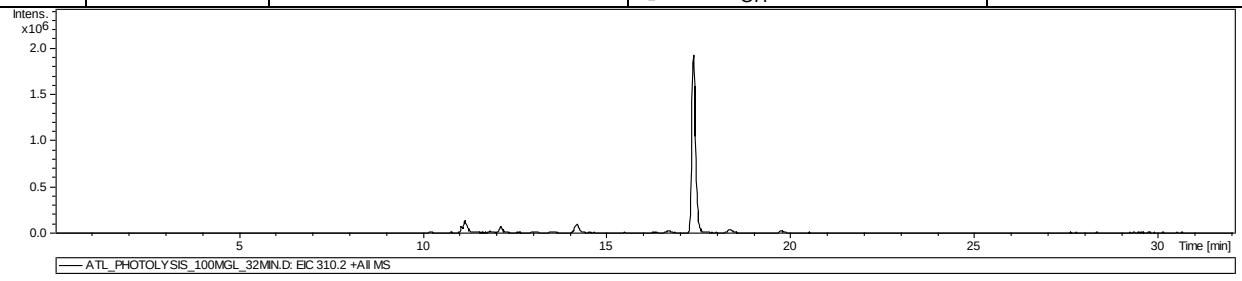

MS^2

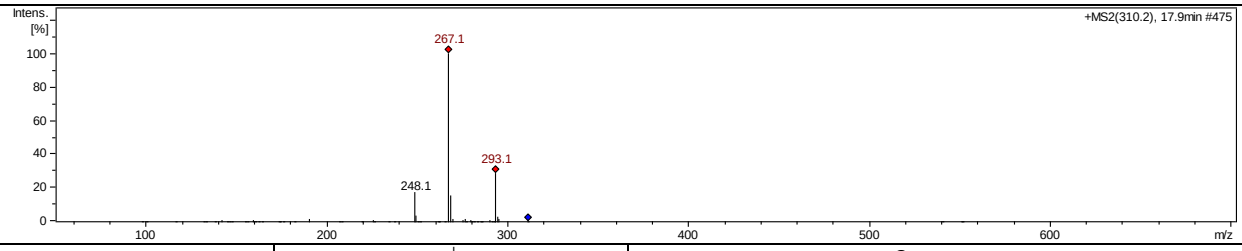

293.1	$[M+H-H_2O]^+$	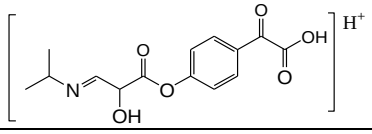
267.1	$[M+H-CH(CH_3)_2]^+$	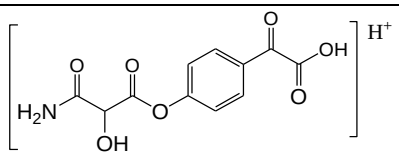
248.1	$[M+H-H_2O-HCOOH]^+$	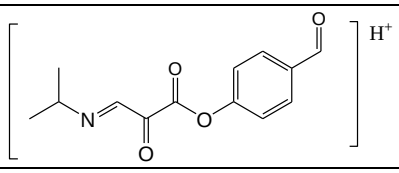

TP 316

m/z	Retention time	Precursor/ Product ion	Structure	References
316.2	13.2	$[M+H]^+$	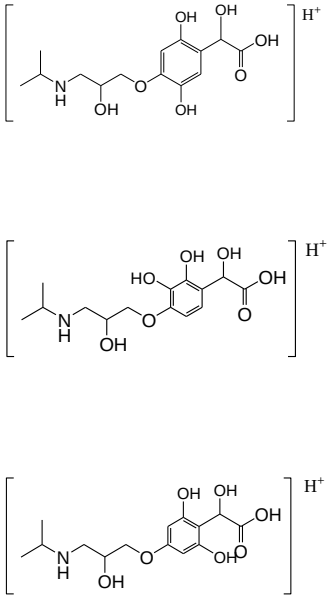	

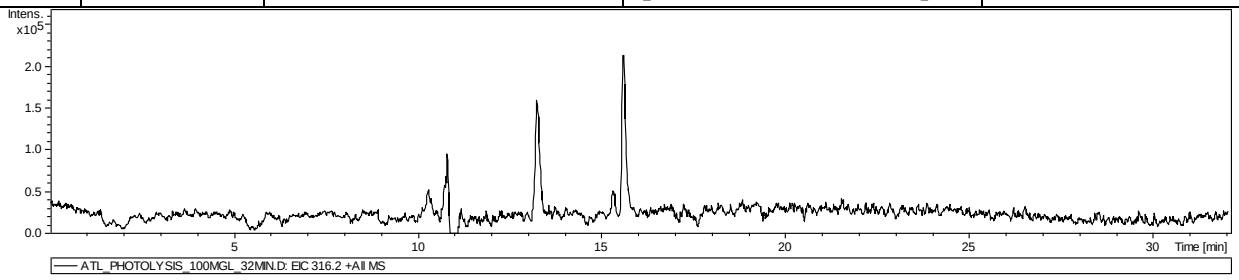

MS^2

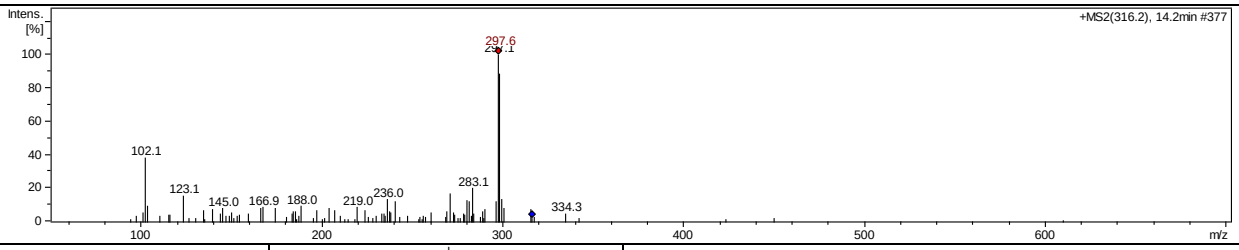

297.6	$[M+H-H_2O]^+$	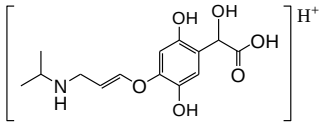
236.0	$[M+H-2H_2O-CH_2(CH_3)_2]^+$	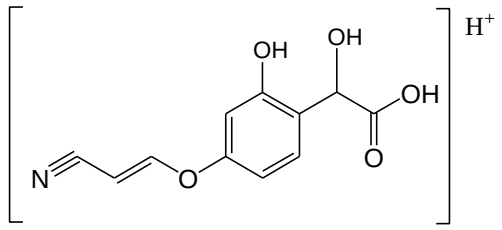

188.0	$[M+H-3H_2O-CH_2(CH_3)_2-HCOOH]^+$	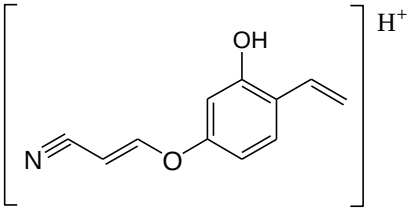
123.1	$[M+H-C_6H_{15}NO_2-H_2O-HCOOH]^+$	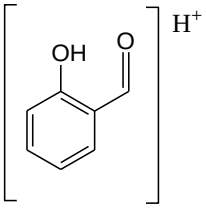
102.1	$[M+H-C_9H_{12}O_6]^+$	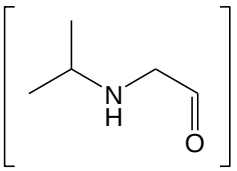

TP 317

m/z	Retention time	Precursor/ Product ion	Structure	References
317.2	17.6	$[M+H]^+$	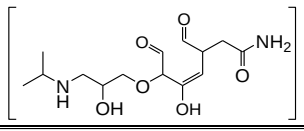	

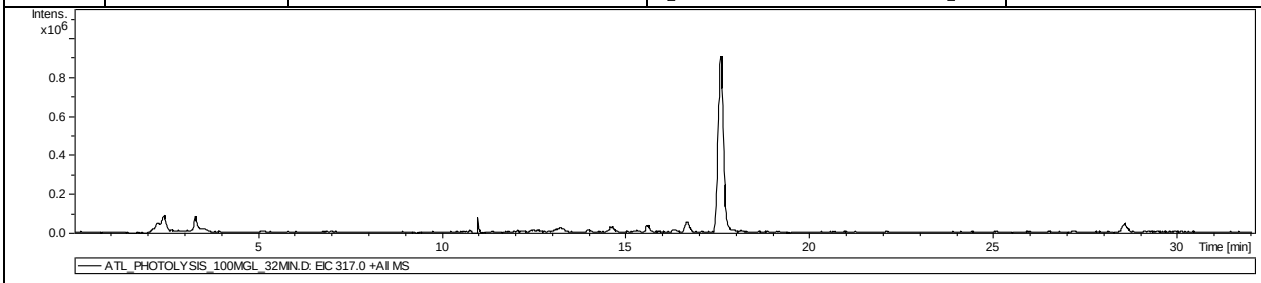

MS^2

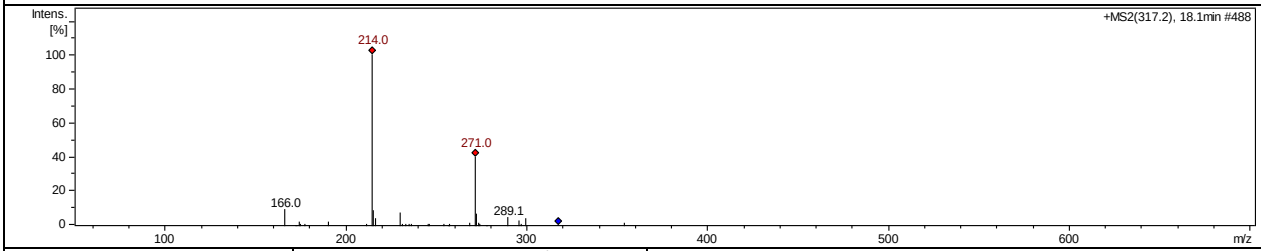

271.0	$[M+H-CH(CH_3)_2]^+$	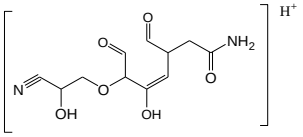
214.0	$[M+H-CH(CH_3)_2-CH_3CONH_2]^+$	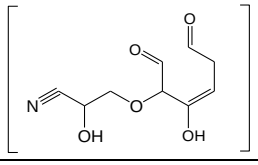

166.0	$[M+H-CH(CH_3)_2-CH_3CONH_2-3H_2O]^+$	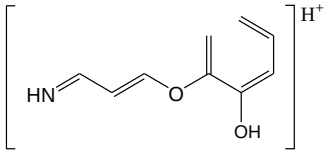

TP 318

m/z	Retention time	Precursor/ Product ion	Structure	References
318.2	12.2	$[M+H]^+$	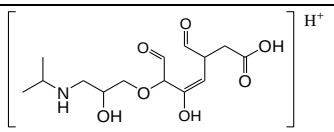	

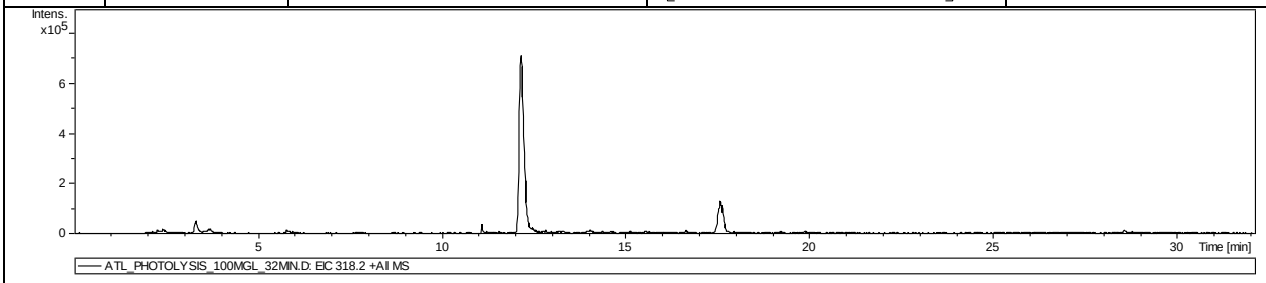

MS^2

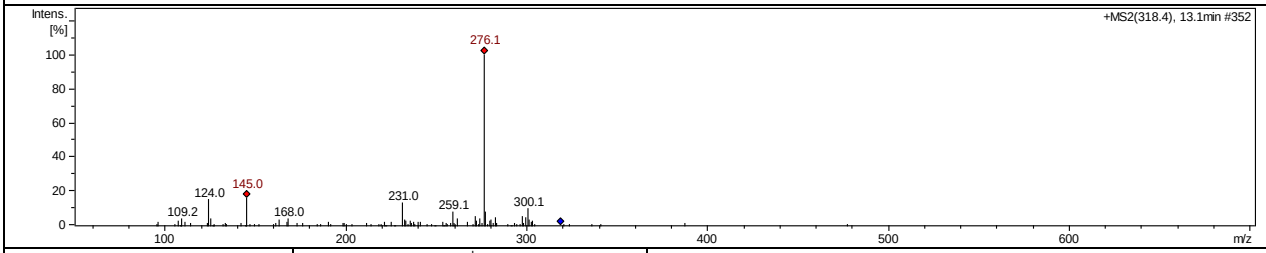

300.1	$[M+H-H_2O]^+$	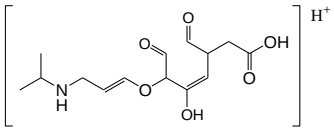
276.0	$[M+H-CH(CH_3)_2]^+$	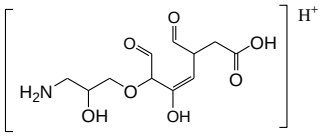
259.1	$[M+H-NH_2CH(CH_3)_2]^+$	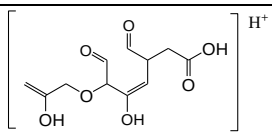
231.0	$[M+H-CH_3NHCH(CH_3)_2-H_2O]^+$	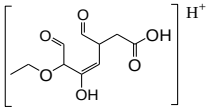
145.0	$[M+H-CH_3NHCH(CH_3)_2-CH_3CH_2OH-CH_3COOH]^+$	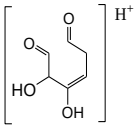
124.0	$[M+H-NH2CH(CH_3)_2-CH_3COOH-2HCHO]^+$	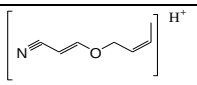

TP 325

m/z	Retention time	Precursor/ Product ion	Structure	References
325.2	12.9min	$[M+H]^+$	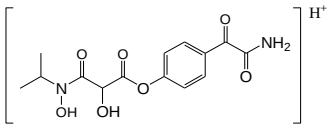	

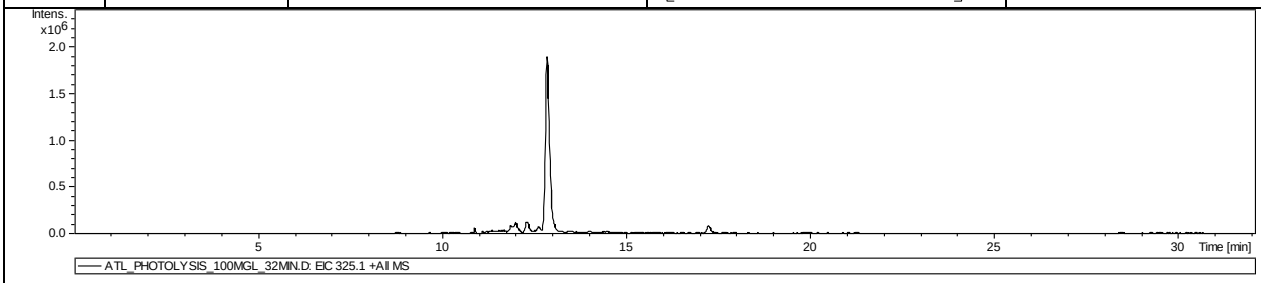

MS^2

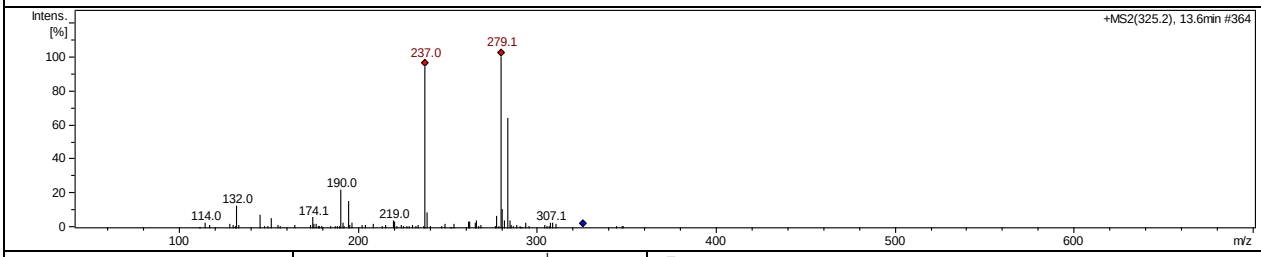

283.0	$[M+H-CH(CH_3)_2]^+$	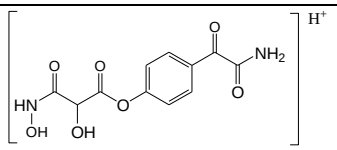
279.1	$[M+H-H_2O-2O]^+$	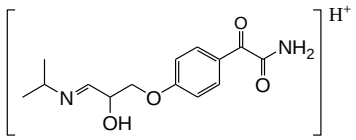
237.0	$[M+H-CH(CH_3)_2-H_2O-2O]^+$	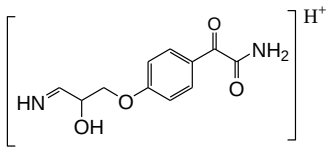
194.0	$[M+H-C_5H_{11}NO_3]^+$	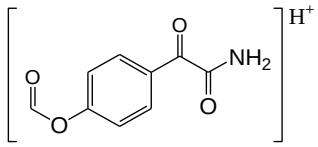
190.0	$[M+H-C_4H_9NO_2-2H_2O]^+$	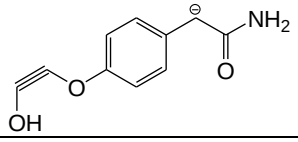
132.0	$[M+H-C_9H_8NO_4]^+$	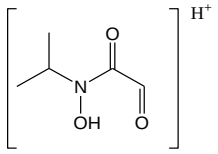

TP 332

m/z	Retention time	Precursor/ Product ion	Structure	References
332.3	13.5 min	$[M+H]^+$	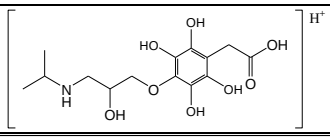	

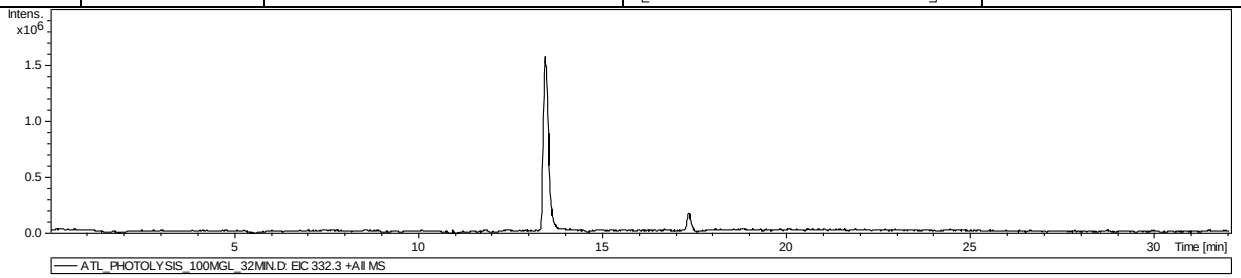

MS^2

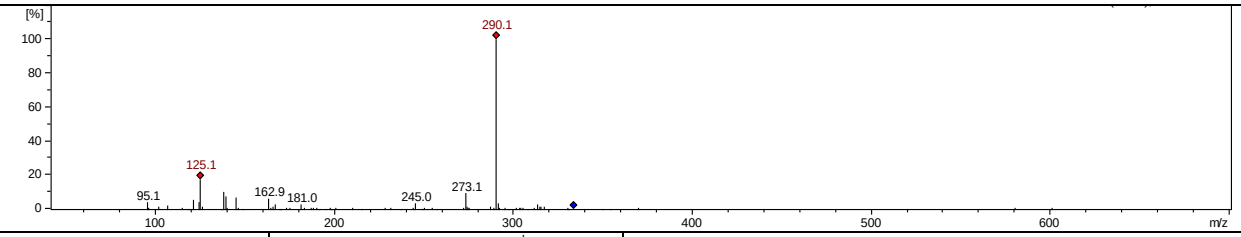

290.1	$[M+H-CH(CH_3)_2]^+$	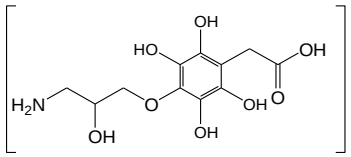
273.1	$[M+H-NH_2CH(CH_3)_2]^+$	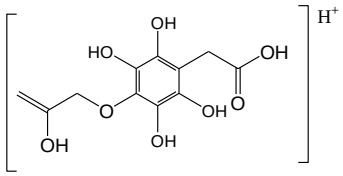
245.0	$[M+H-CH_3NHCH(CH_3)_2-H_2O]^+$	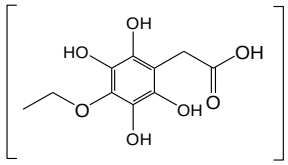

TP 336

m/z	Retention time	Precursor/ Product ion	Structure	References
336.3	14.8 min	$[M+H]^+$	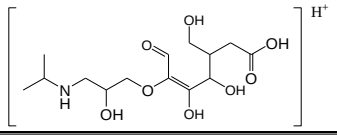	

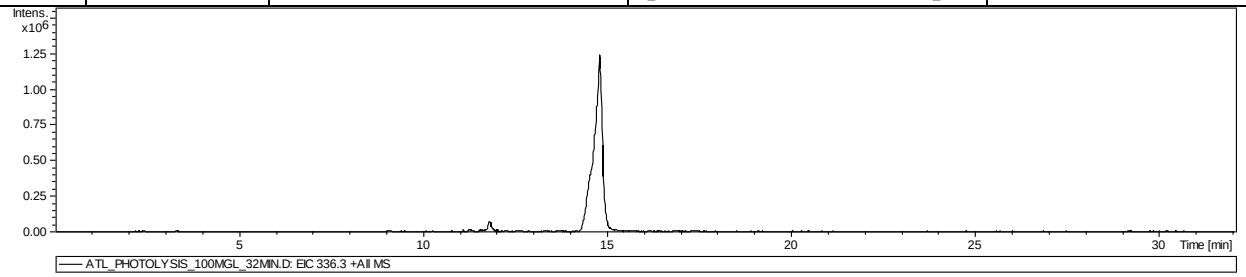

MS^2

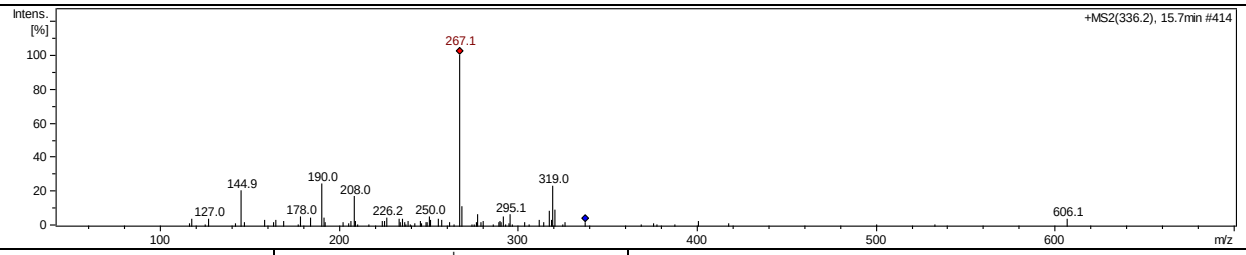

319.0	$[M+H-H_2O]^+$	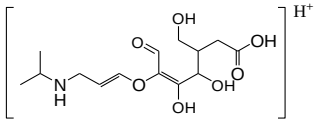
267.0	$[M+H-NH_2CH(CH_3)_2-O]^+$	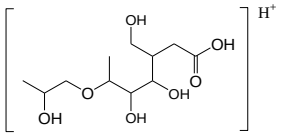
208.0	$[M+H-CH(CH_3)_2-CH_3COOH-HCHO]^+$	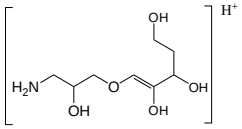
190.0	$[M+H-CH(CH_3)_2-CH_3COOH-HCHO-H_2O]^+$	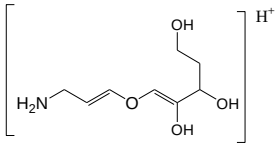
144.9	$[M+H-NH_2CH(CH_3)_2-CH_3COOH-HOCH_2CH_2CH_2OH]^+$	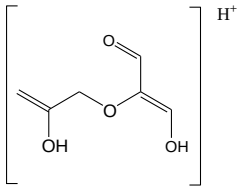
127.0	$[M+H-NH_2CH(CH_3)_2-CH_3COOH-HOCH_2CH_2CH_2OH-H_2O]^+$	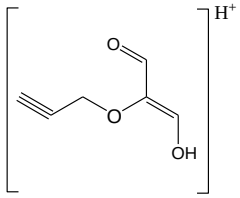

TP 387

m/z	Retention time	Precursor/ Product ion	Structure	References
387.1	12.0 min	$[M+H]^+$	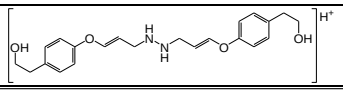	27

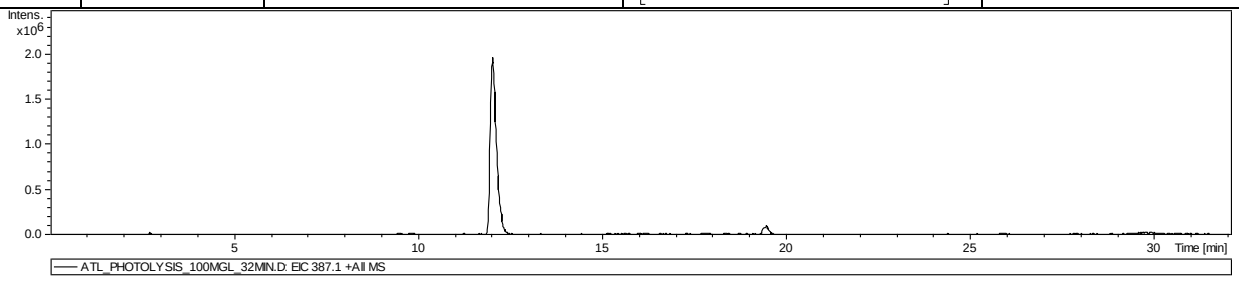

MS^2

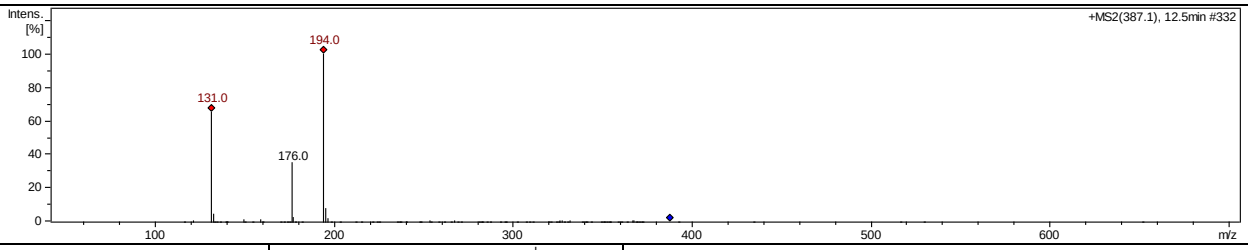

194.0	$[M+H-C_{11}H_{15}NO_2]^+$	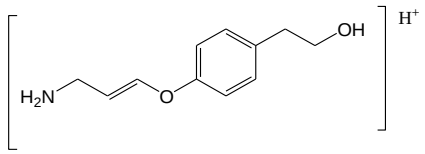
176.0	$[M+H-C_{11}H_{15}NO_2-H_2O]^+$	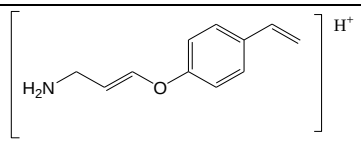
131.0	$[M+H-C_{11}H_{15}NO_2-CH_3OH-CH_3NH_2]^+$	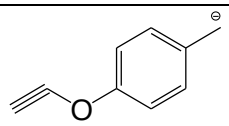

TP 419

m/z	Retention time	Precursor/ Product ion	Structure	References
419.1	14.6 min	$[M+H]^+$	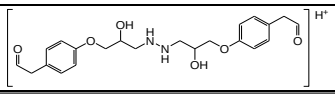	27

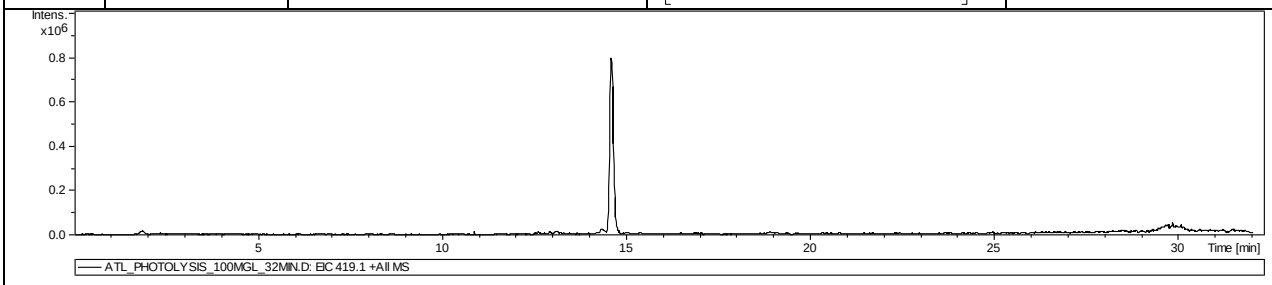

MS^2

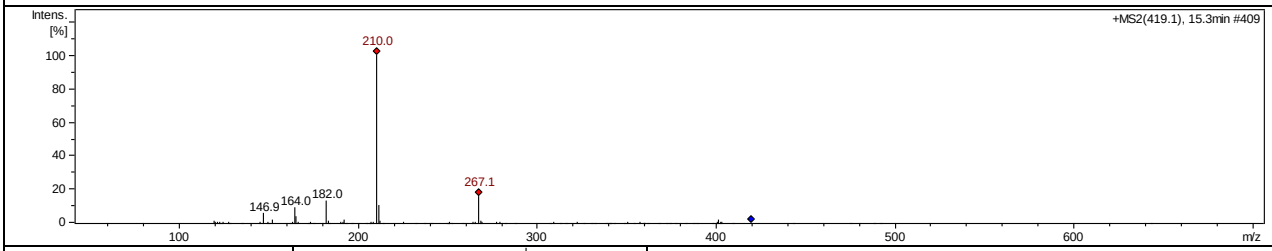

267.0	$[M+H-C_9H_{12}O_2]^+$	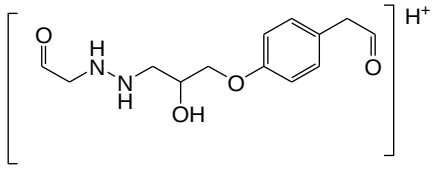
210.0	$[M+H-C_{11}H_{15}NO_3]^+$	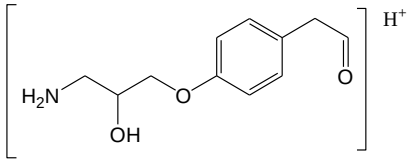
182.0	$[M+H-C_{11}H_{15}NO_3\text{-}HCHO]^+$	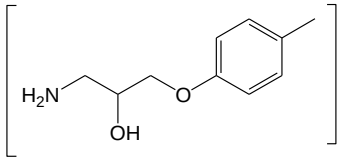
164.0	$[M+H-C_{11}H_{15}NO_3\text{-}HCHO\text{-}H_2O]^+$	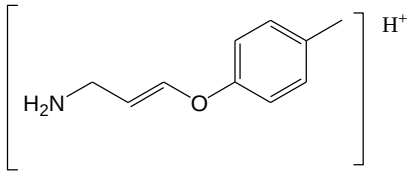

Table S9 Supporting Information: QSAR predictions for Atenolol and its derivatives (photo-TPs) for biodegradability different models- 1: CATABOL 301C model under MITI test condition, 2: CATALOGIC 301C model; 3: BioWin 6 (non-linear model) for MITI Biodegradation probability; 4: Case Ultra-Readily biodegradability under MITI test (OECD 301C); bonds and hetero atoms in bold: structural alerts as provided by Case Ultra

	QSAR models				**Multicase activating and deactivating alerts highlighted**		
Derivatives	**1**[§]	**2**[§]	**3**[‡]	**4**	**Activating alert**	**Deactivating alert**	**Unknown fragment**
Atenolol	0.3168	0.4445	0.235	Inconclusive*	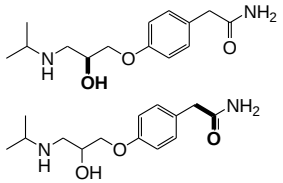	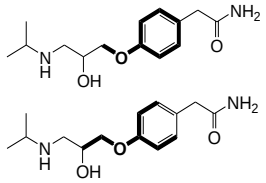	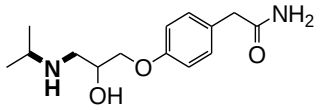
TP 134	0.5375	0.7462	0.751	+	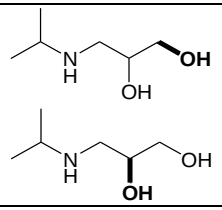		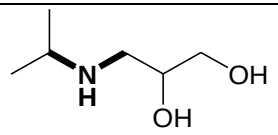
TP_1 151	0.0230	0.0298	0.765	-		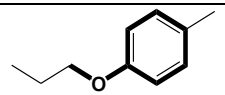	
TP_2 151	0.8113	0.8360	0.802	+	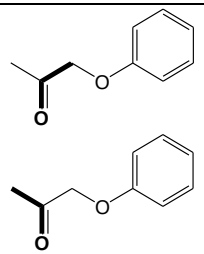		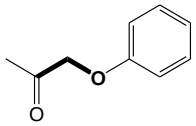
TP 152	0.6327	0.5554	0.473	+	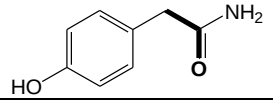		

TP 176	0.2742	0.2626	0.391	Inconclusive	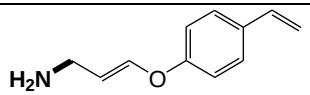		
TP 193	0.2110	0.2072	0.269	Inconclusive	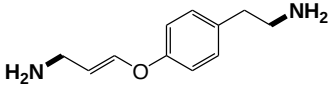		
TP 194	0.2493	0.2479	0.565	Inconclusive	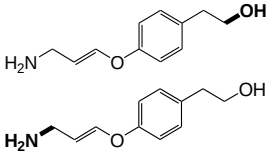		
TP 207	0.4173	0.6278	0.351	Inconclusive	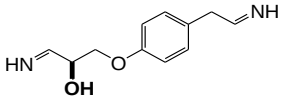	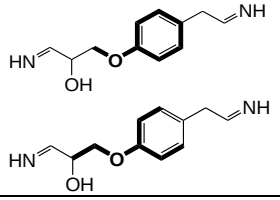	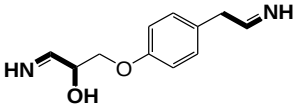
TP 210	0.3108	0.4270	0.916	Inconclusive*	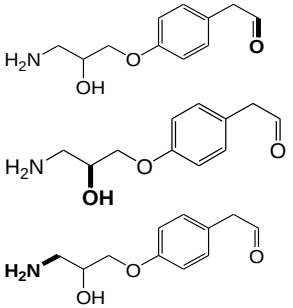	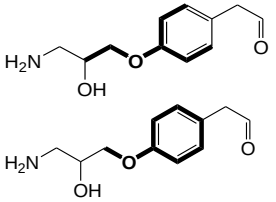	
TP 223	0.3423	0.5465	0.477	Inconclusive*	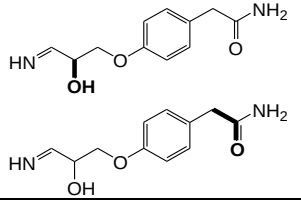	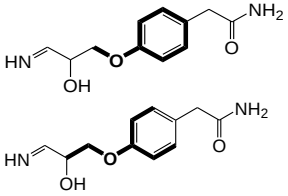	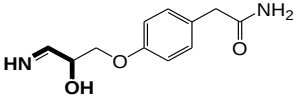
TP 225	0.2594	0.3897	0.524	Inconclusive*	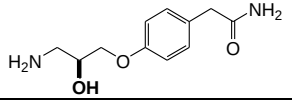	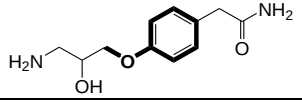	

					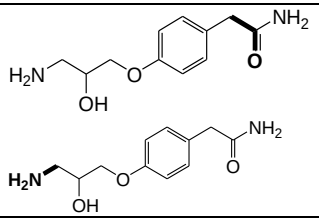	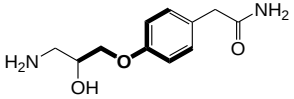	
TP 232	0.3363	0.3789	0.524	Inconclusive	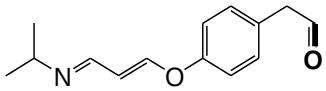	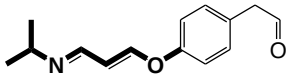	
TP 238	0.4097	0.5552	0.838	Inconclusive*	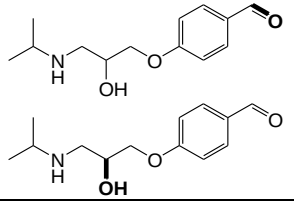	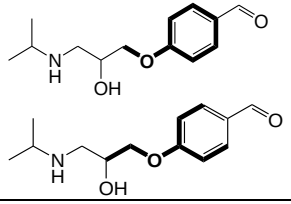	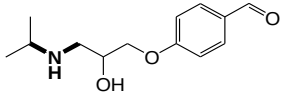
TP 249	0.2473	0.2970	0.126	Inconclusive	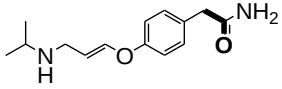		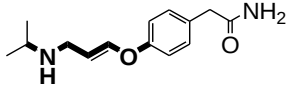
TP 253	0.5645	0.5914	0.673	+	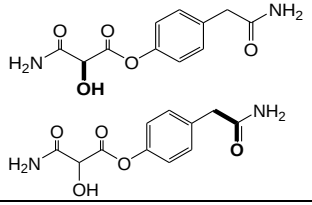		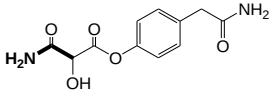
TP_1 254	0.4300	0.5588	0.824	Inconclusive*	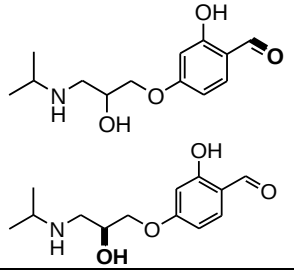	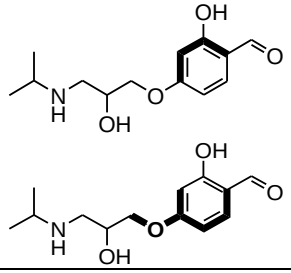	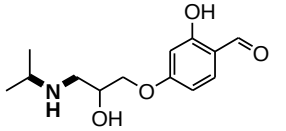

						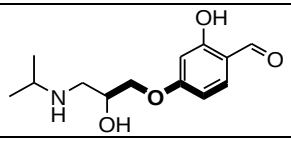	
TP_2 254	0.4316	0.5764	0.824	Inconclusive*	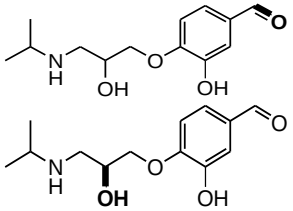	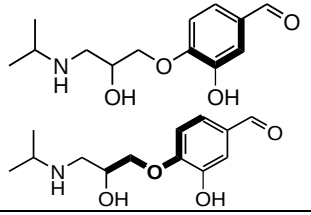	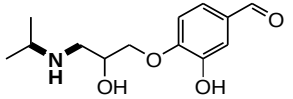
TP 265	0.3168	0.4445	0.233	±	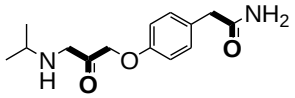	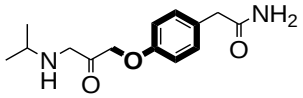	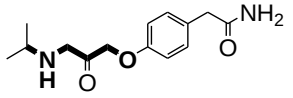
TP 275	0.6058	0.6427	0.679	Inconclusive*	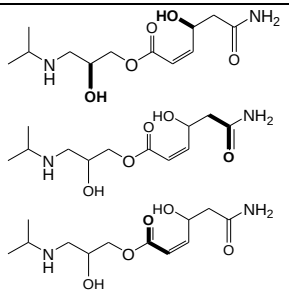	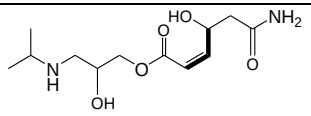	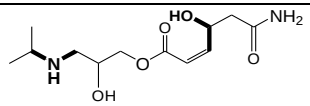
TP_1 281	0.3320	0.4625	0.216	±	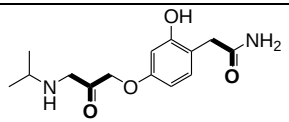	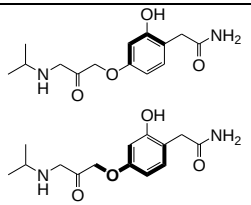	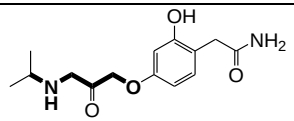
TP_2 281	0.3348	0.4998	0.216	±	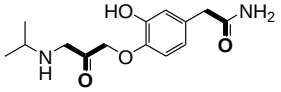	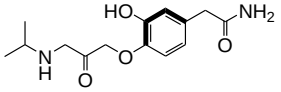	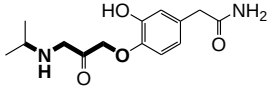
TP_3 281	0.3207	0.4087	0.434	Inconclusive	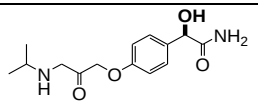	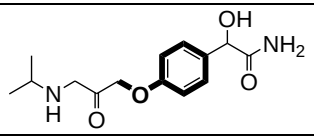	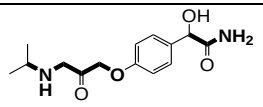

					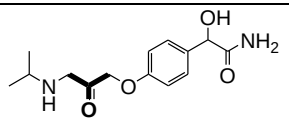		
TP_4 281	0.5935	0.6340	0.235	±	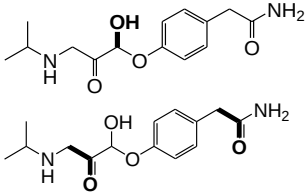		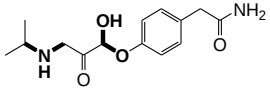
TP_5 281	0.3484	0.4995	0.235	Inconclusive	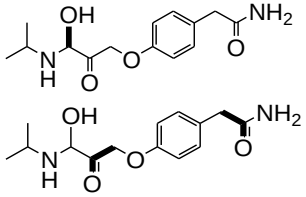	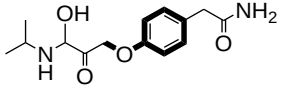	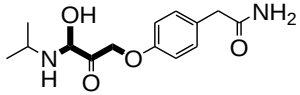
TP_1 283	0.3320	0.4625	0.219	Inconclusive*	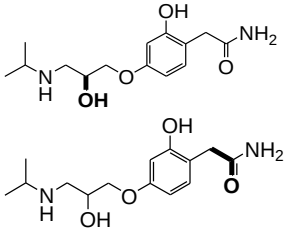	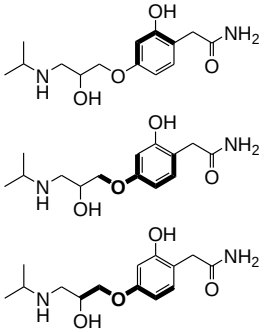	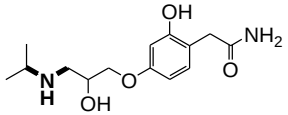
TP_2 283	0.3348	0.4998	0.219	Inconclusive*	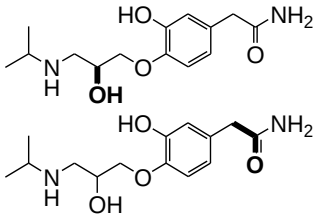	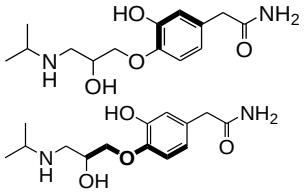	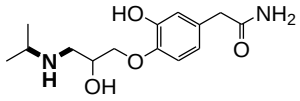

TP_3 283	0.3207	0.4087	0.437	Inconclusive*	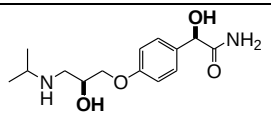	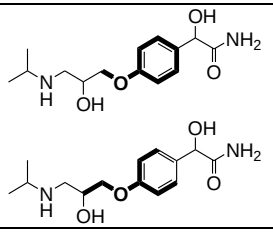	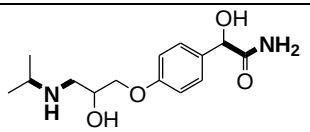
TP_4 283	0.5935	0.6340	0.237	+	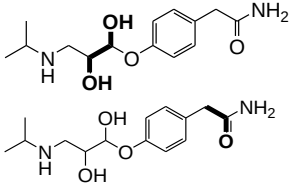		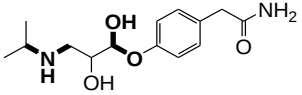
TP_5 283	0.3484	0.4977	0.237	Inconclusive*	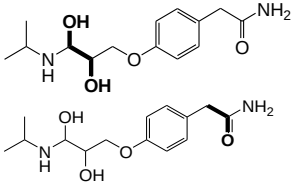	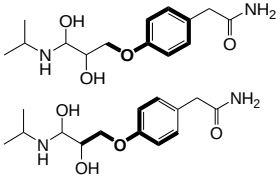	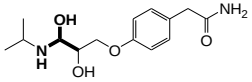
TP_6 283	0.2974	0.4255	0.443	Inconclusive*	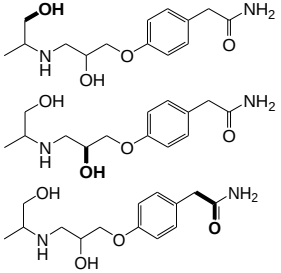	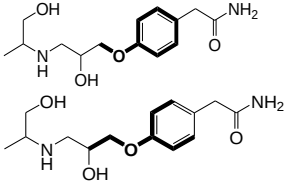	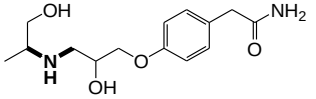
TP_7 283	0.3484	0.4720	0.242	Inconclusive	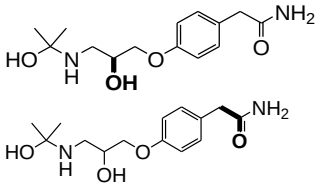	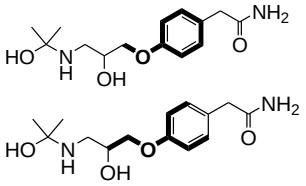	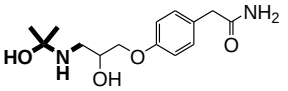
TP 285	0.3773	0.4178	0.196	Inconclusive	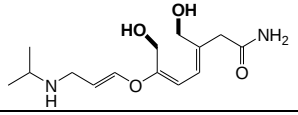		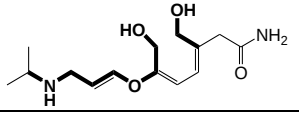

					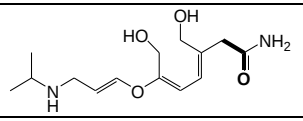		
TP 287	0.6029	0.6565	0.895	Inconclusive*	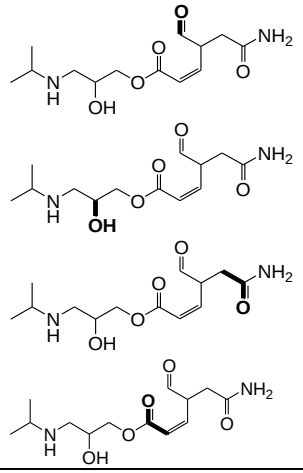	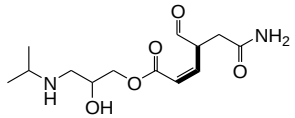	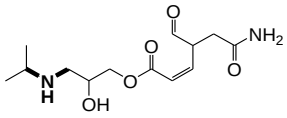
TP_1 295	0.4790	0.5279	0.365	+	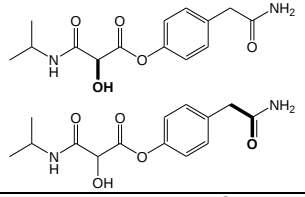		
TP_2 295	0.2144	0.3712	0.246	Inconclusive*	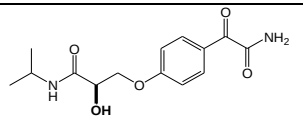	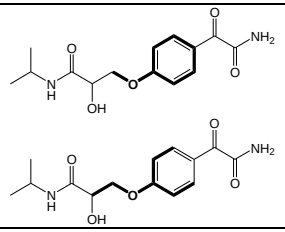	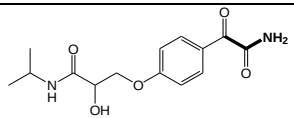
TP_1 297	0.3408	0.4719	0.175	Inconclusive*	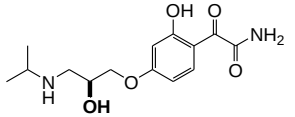	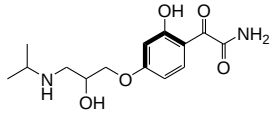	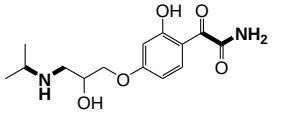

						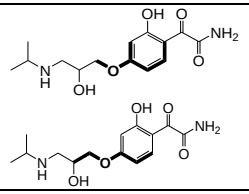	
TP_2 297	0.2372	0.3734	0.282	Inconclusive*	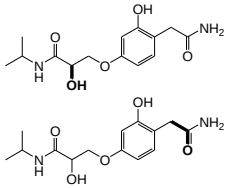	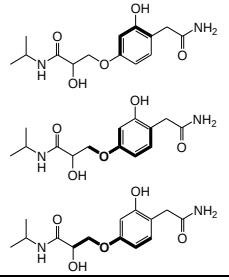	
TP 299	0.3521	0.5297	0.203	Inconclusive*	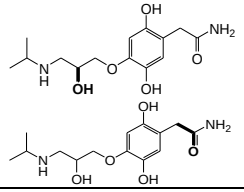	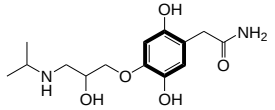	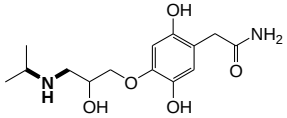
TP_1 301	0.4161	0.4743	0.672	+	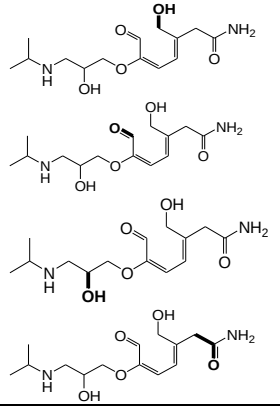		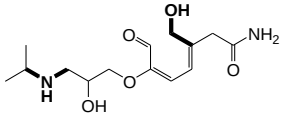
TP_2 301	0.3538	0.3786	0.553	Inconclusive*	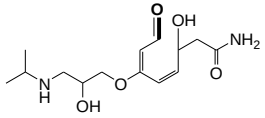	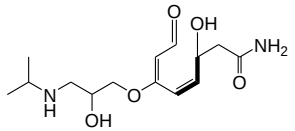	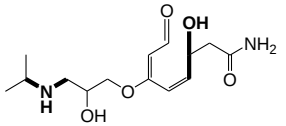

					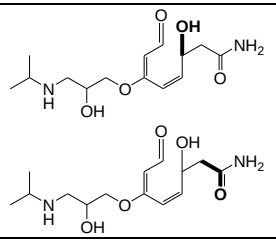		
TP_3 301	0.7786	0.8535	0.553	Inconclusive	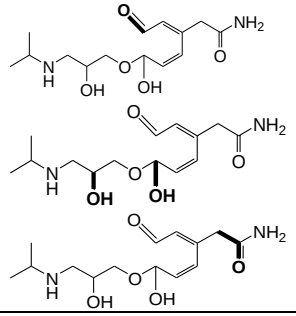	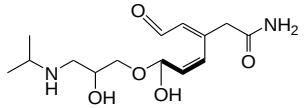	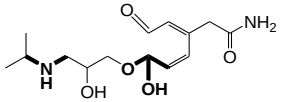
TP_4 301	0.4663	0.6603	0.672	Inconclusive	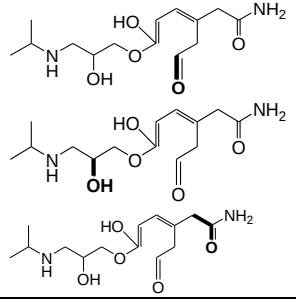		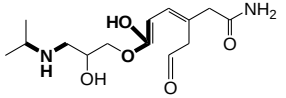
TP_5 301	0.3538	0.3786	0.553	Inconclusive*	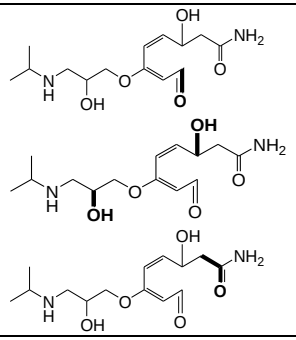	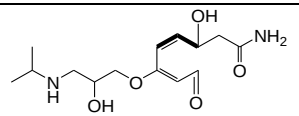	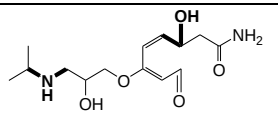

TP_6 301	0.4161	0.4743	0.672	+	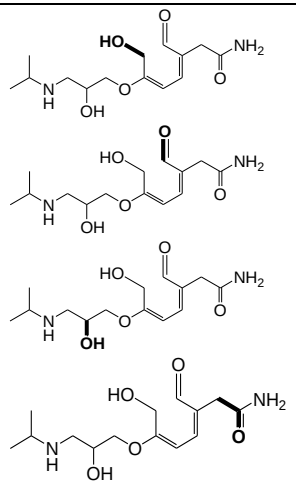		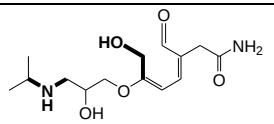
TP_1 309	0.2678	0.4518	0.96	Inconclusive	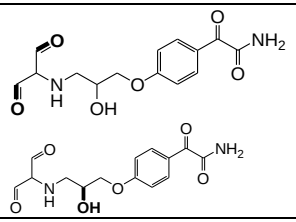	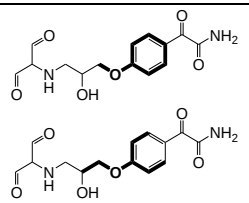	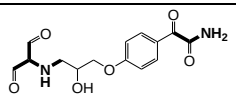
TP_2 309	0.3888	0.5348	0.303	+	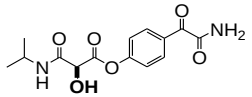		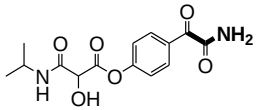
TP 310	0.6000	0.6979	0.352	+	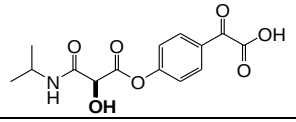		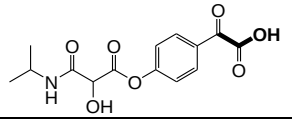
TP_1 316	0.3044	0.5433	0.446	Inconclusive*	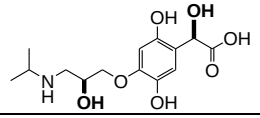	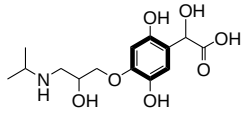	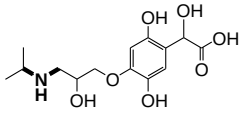
TP_2 316	0.2973	0.5039	0.446	Inconclusive*	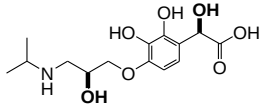	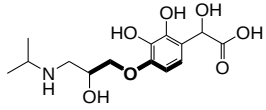	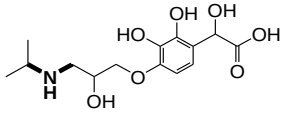

TP_3 316	0.2914	0.5071	0.446	Inconclusive*	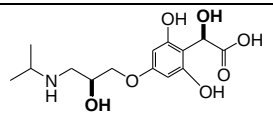	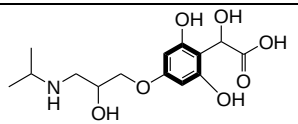	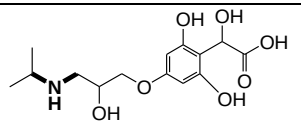
TP 317	0.2919	0.5230	0.912	+	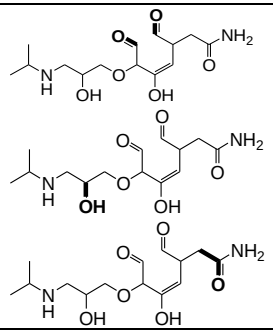		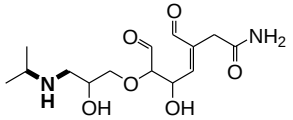
TP 318	0.3137	0.6750	0.928	±	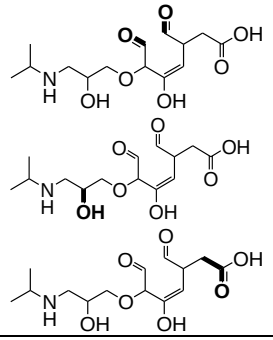		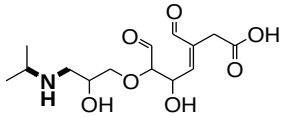
TP 325	0.3888	0.5348	0.102	Inconclusive	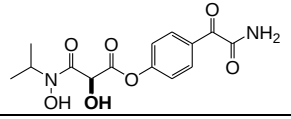		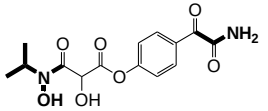
TP 332	0.4295	0.5857	0.208	±	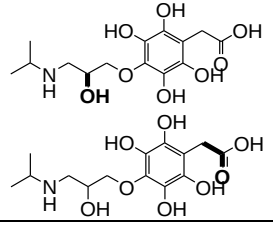		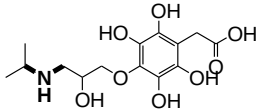

TP 336	0.3661	0.5533	0.846	Inconclusive	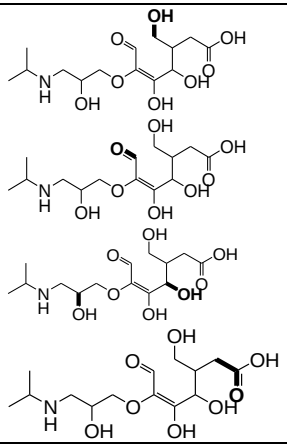		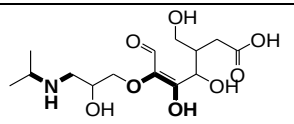
TP 387	0.1945	0.1613	0	Inconclusive	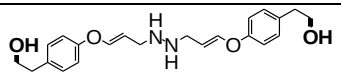		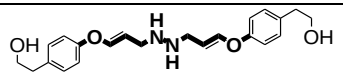
TP 419	0.0612	0.0981	0	Inconclusive*	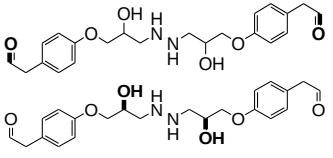	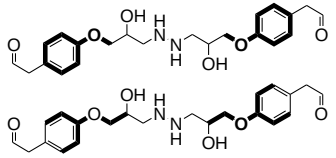	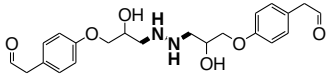

§: “100% biodegradation” was assigned a numeric value of 1 and “0% biodegradation” was assigned a numeric value of 0. ‡: “Readily biodegradable" was assigned a numeric value of 1 and “not readily biodegradable" was assigned a numeric value of 0. (0 to 1 is the probability range to undergo biodegradation). Out of Domain [OD] means that the test chemical is not included in the applicability domain of the model used. ‘Inconclusive’ means a significant portion of the test chemical is covered by unknown structural fragments. Inconclusive with asterisk symbol (*) means both positive and deactivating alerts were found in the same molecule and therefore a clear result cannot be provided. + : a positive alert for corresponding activity; - : a negative alert for corresponding activity ; ±: positive alert with low signal (marginal positive) for corresponding activity.

Table S10 Supporting Information: *In silico* toxicity prediction by different QSAR models of Case Ultra, Leadscope and OASIS Catalogic for Atenolol and its biodegradable derivatives (photo-TPs)

Derivatives	CASE Ultra					Leadscope				OASIS Catalogic V.5.11.6
	A (A0J)	B (A7S)	C (A7U)	D (AUA)	E (A2H)	B	C	E	F	E
Atenolol	-	§*	-	OD	-	-	+	-	-	-
TP 176	±	OD	OD	‡*	-	OD	OD	-	+	+
TP 193	±	OD	OD	‡*	-	OD	-	-	+	+
TP 194	±	OD	OD	‡*	+	OD	OD	-	+	+
TP 207	OD	OD	OD	OD	OD	-	-	-	-	-
TP 210	-	-	-	-	-	-	+	-	-	-
TP 223	OD	§*	-	OD	-	-	OD	-	-	-
TP 225	OD	§*	-	-	-	-	+	-	-	-
TP 238	-	-	-	OD	-	-	+	-	-	-
TP_1 283	-	§*	-	OD	-	-	+	-	-	-

TP_2 283	§*	+	-	OD	-	-	+	-	-	-
TP_3 283	-	§*	-	OD	-	-	+	-	-	-
TP_4 283	-	+	-	OD	-	-	+	-	-	-
TP_5 283	OD	§*	-	OD	-	-	+	-	-	-
TP_6 283	-	§*	-	OD	-	-	-	-	-	-
TP_7 283	OD	§*	-	OD	-	-	+	-	-	-
TP_1 295	+	+	-	-	-	OD	OD	-	OD	-
TP_2 295	+	§*	-	+	-	-	+	-	+	-
TP 299	-	+	-	OD	-	-	+	-	-	-
TP_1 301	-	+	-	‡*	§*	-	+	-	-	-
TP_2 301	-	+	-	‡*	-	-	+	-	-	-
TP_3 301	OD	+	-	‡*	-	-	+	-	-	-
TP_4 301	OD	+	OD	‡*	-	-	+	-	-	-
TP_5 301	-	+	-	‡*	-	-	+	-	-	-
TP_6 301	-	+	-	‡*	§*	-	+	-	-	-
TP_2 309	+	+	-	+	-	-	+	-	+	-

TP 317	OD	+	-	OD	-	-	+	-	-	-
TP 318	OD	-	-	OD	-	-	+	-	-	-
TP 325	+	+	OD	+	-	-	+	-	+	-
TP 332	-	+	-	OD	-	-	+	-	-	-

A- Human carcinogenicity; B- Micronucleus in vivo composite; C- Chromosome aberration in vitro CHO cells; D- Microtox against environmental bacteria; E- Salmonella Mutagenicity; F- Mammalian Mutagenicity; OD: Out of Domain means that the test chemical is not included in the applicability domain of the applied model; §*: Inconclusive with asterisk symbol (*) means both positive and deactivating alerts were found in the same molecule and therefore a clear result cannot be provided; §: Inconclusive means that the molecule contained too many unknown fragments; + : a positive alert for corresponding activity; - : a negative alert for corresponding activity; ±: Marginal positive; ‡* : positive alert with low statistical significance.

Reference

1. W. M. M. Mahmoud, C. Trautwein, C. Leder and K. Kümmerer, *Sci. Total Environ.*, 2013, **463–464**, 140.
2. T. Rastogi, C. Leder and K. Kümmerer, *Sci. Total Environ.*, 2014, **482–483**, 378.
3. ISO 8245, *Water quality -- Guidelines for the determination of total organic carbon (TOC) and dissolved organic carbon (DOC)*, 1999.
4. OECD, *OECD Guidelines for the Testing of Chemicals: Ready Biodegradability 301D: Closed Bottle Test*, OECD Pub., 1992.
5. OECD, *OECD Guidelines for the Testing of Chemicals: Ready Biodegradability 301F: Manometric Respiratory Test*, OECD Pub., 1992.
6. J. Friedrich, A. Längin and K. Kümmerer, *CLEAN – Soil, Air, Water*, 2013, **41**, 251.
7. OECD, *Revised introduction of the OECD guidelines for testing of chemicals, Section 3*, Organisation of Economic Cooperation and Development, 2006.
8. N. Nyholm, *Environ. Toxicol. Chem.*, 1991, **10**, 1237.
9. A. Sedykh, R. Saiakhov and G. Klopman, *Chemosphere*, 2001, **45**, 971.
10. G. Roberts, G. Myatt, W. Johnson, K. Cross and P. Blower, *J. Chem. Inf. Model.*, 2000, **40**, 1302.
11. W. M. M. Mahmoud, A. P. Toolaram, J. Menz, C. Leder, M. Schneider and K. Kümmerer, *Water Research*, 2014, **49**, 11.
12. S. K. Chakravarti, R. D. Saiakhov and G. Klopman, *J. Chem. Inf. Model.*, 2012, **52**, 2609.
13. EPA, "OPPT/Exposure Assessment Tools and Models/Estimation Program Interface (EPI) Suite Version 3.12, http://www.epa.gov/oppt/exposure/pubs/episuite.htm, 2013.
14. Laboratory of Mathematical Chemistry Bulgaria, *OASIS Catalogic software V.5.11.6TB*, 2012.
15. R. Saiakhov, S. Chakravarti and G. Klopman, *Mol. Inf.*, 2013, **32**, 87.
16. W. L. Jorgensen, *Small-Molecule Drug Discovery Suite 2013-3: QikProp*, Schrödinger, New York, 2013.
17. W. L. Jorgensen, "QikProp 3.8. User Manual", http://helixweb.nih.gov/schrodinger-2013.3-docs/qikprop/qikprop_user_manual.pdf, 2014.
18. C. A. Lipinski, F. Lombardo, B. W. Dominy and P. J. Feeney, *Advan. Drug Delivery Rev.*, 2001, **46**, 3.
19. V. Andrisano, R. Gotti, A. Leoni and V. Cavrini, *J. Pharm. Biomed. Anal.*, 1999, **21**, 851.
20. C. Medana, P. Calza, F. Carbone, E. Pelizzetti, H. Hidaka and C. Baiocchi, *Rapid Commun. Mass Spectrom.*, 2008, **22**, 301.
21. J. Radjenovic, C. Sirtori, M. Petrovic, D. Barceló and S. Malato, *Applied Catalysis B: Environ.*, 2009, **89**, 255.
22. E. Marco-Urrea, J. Radjenović, G. Caminal, M. Petrović, T. Vicent and D. Barceló, *Water Research*, 2010, **44**, 521.

23. E. Isarain-Chavez, C. Arias, P. L. Cabot, F. Centellas, R. M. Rodriguez, J. A. Garrido and E. Brillas, *Applied Catalysis B: Environ.*, 2010, **96**, 361.
24. K. S. Tay, N. A. Rahman and M. R. B. Abas, *Microchem. J.*, 2011, **99**, 312.
25. Y. Chen, H. Li, Z. Wang, H. Li, T. Tao and Y. Zuo, *Water Research*, 2012, **46**, 2965.
26. Y. Ji, L. Zhou, C. Ferronato, X. Yang, A. Salvador, C. Zeng and J.-M. Chovelon, *J. Photochem. Photobiol. A: Chem.*, 2013, **254**, 35.
27. M. L. Wilde, W. M. M. Mahmoud, K. Kümmerer and A. F. Martins, *Sci. Total Environ.*, 2013, **452–453**, 137.
28. Y. Ji, C. Zeng, C. Ferronato, J.-M. Chovelon and X. Yang, *Chemosphere*, 2012, **88**, 644.
29. V. Kumar, R. P. Shah, S. Malik and S. Singh, *J. Pharma. Biomed. Anal.*, 2009, **49**, 880.